

3. RESULTS

3.1 Bioinformatics analysis for *MoSKP1*

Bioinformatics analysis was done to find *Skp1* homologue in *M. oryzae*, using BROADmit database (http://www.broadinstitute.org/annotation/genome/magnaporthe_grisea/MultiHome.html). A single hit was obtained from a putative *MoSKP1* (MGG_04978) gene sequence. *MoSKP1* (MGG_04978) was then taken as query and searched in GROMO (http://gromo.msubiotech.ac.in/Gromo/Complete_Search.cgi) to obtain general information about the gene. Information like gene length, protein sequence (169aa), molecular weight (19.3kD) was obtained. This protein has negative charge of -14 and isoelectric point of 4.276. *MoSKP1* domain search was done using the NCBI (<http://www.ncbi.nlm.nih.gov/Structure/cdd/wrpsb.cgi?RID=ZUK06AWJ01N&mode=all>) the sequence is predicted to have dimerisation and tetramerisation domain indicating that the protein is functional in a multiprotein complex (Fig. 7b). The homology of *MoSKP1* with budding yeast indicates the presence of kinetochore domain in *MoSKP1*. Budding yeast *Skp1* contains kinetochore domain at C-terminal region and involve in kinetochore assembly and required for cell cycle progression (Connely and Hieter 1996). The presence of superfamily BTB/POZ domain was also observed near to the N-terminus of *MoSkp1* protein sequence. The BTB (BR-C, ttk and bab)/POZ (Pox virus and Zinc finger) domain mediates homomeric dimerisation and in some instances heteromeric dimerisation. POZ domains from several zinc finger proteins have been shown to mediate transcriptional repression and to interact with components of histone deacetylase co-repressor complexes including N-CoR and SMRT.

A multiple sequence alignment was done using *Magnaporthe oryzae*, *Fusarium oxysporum*, *S. pombe*, Human and *S. cerevisiae*, having accession numbers MGG_04978, AAT85970, CAB52607, AAH20798, AAB17500 respectively, to analyse how the sequences are conserved across species. The similarity at protein level indicated that all these proteins may have similar functions *in vivo*. To evaluate the relative distance of *Magnaporthe* with other *Ascomycetous* members, a nucleotide BLAST was performed using *M. oryzae* MGG_04978 sequence as query and sequences were selected showing up to 60% identity at protein level for multiple sequence alignment. The dendrogram shows that *Magnaporthe* is closer to *Neurospora crassa*. It is clear from the evolutionary tree that *F. oxysporum* is very distant from *M. oryzae* Skp1 whereas *S. pombe* and *S. cerevisiae* are closer to MoSkp1, which gives an opportunity to perform interspecies gene complementation with these model systems. Multiple sequence alignment was done using ClustalX 2.0.11 software (Fig. 7) whereas the dendrogram was made by using Mega4 software (Fig. 8).

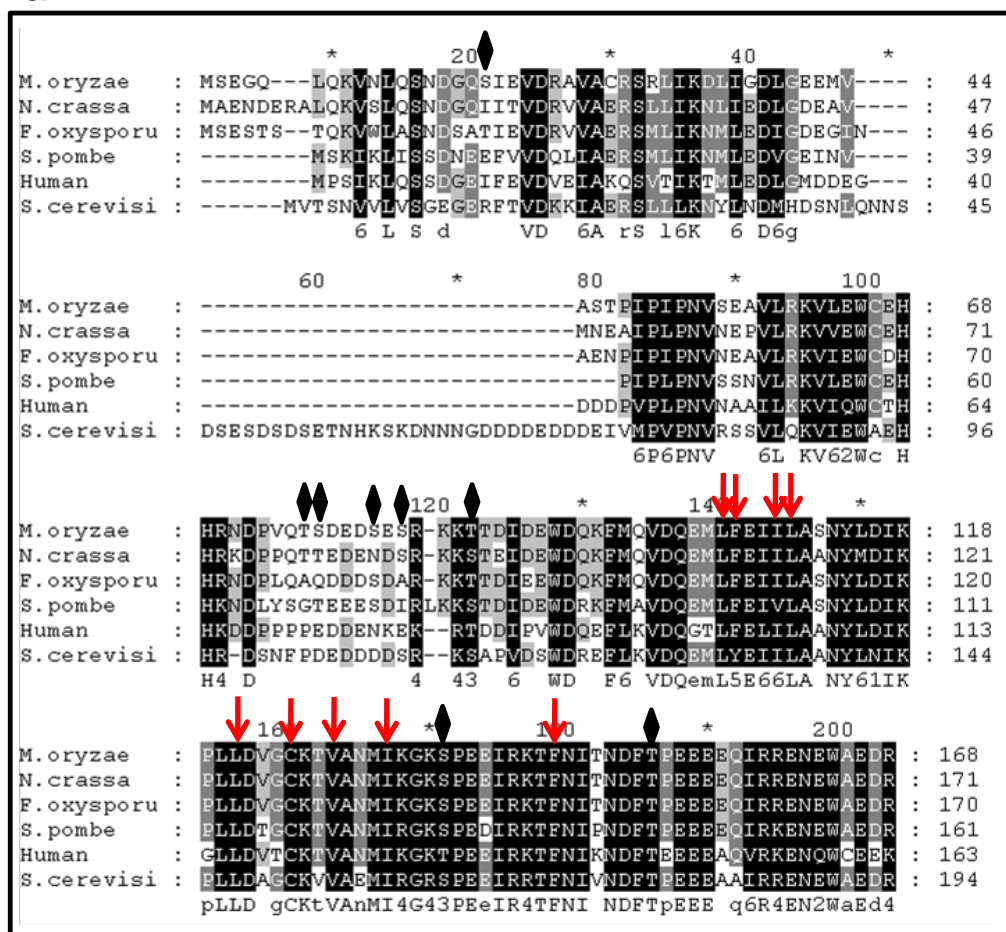
Sequence analysis of *MoSKP1* reveals the presence of potential phosphorylation sites and a dimerisation domain, indicating that protein is functional after oligomerisation and phosphorylation. Phosphorylation site prediction in *M. oryzae* Skp1 was performed using NetPhos 2.0 Yeast tool at ExPASy. This gave several hits, most of which were on serine residues. Of those five Residues, Ser¹⁸, Ser⁷⁷, Ser⁸¹, Ser⁸³ and Ser¹³⁶ having scores of 0.983, 0.998, 0.995, 0.996 and 0.998 respectively, three residues at position 77, 81 and 83 were the most probable targets for phosphorylation (Fig. 8). There are three phosphorylation sites for threonine of which, two are present in the vicinity of serine residue at 76 and 86 position with score 0.993 and 0.794 respectively. The presence of

phosphorylation sites in vicinity to each other possibly will be necessary for the function of MoSKP1.

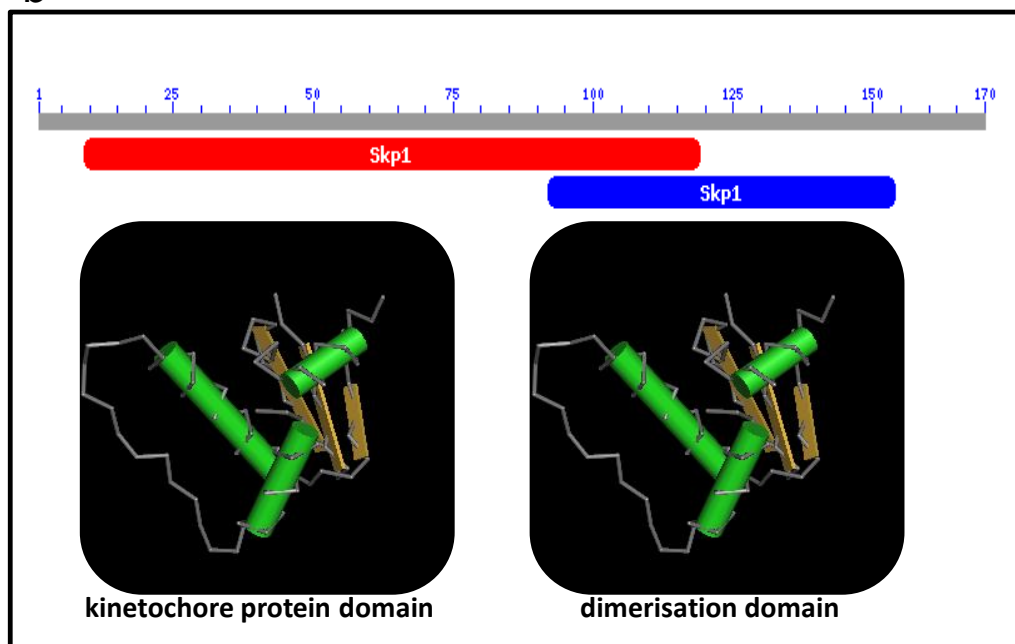
Skp1 is able to bind to a subset of F-box proteins, which is a characteristic feature of the family. Previous report is that Skp1 bind F-box protein by interacting with L1 loop and H1 helix of F-box. On the basis of crystal structure it has been shown that Human Skp1 has 8 α -helix and 3 β -sheets involved in binding to F-box proteins, which contain L1 loop and H1, H2, and H3 helices at the N-terminus. The three helices H5, H6 and H7 of Skp1 present at C-terminus are involved in binding with H1, H2 and H3 helices and L1 loop of F-box proteins. The most extensive contacts are made by the L1 loop and H1 helix of the F-box with H5, H6 and H7 helices of Skp1. From the F-box L1 loop, Trp 109, Leu 112 and Pro 113 contact **Leu 100, Phe 101, Ile 104, Leu 105, Val 123** and **Phe 139** of Skp1. From the F-box H1 helix, Leu 116, Ile 120 and Leu 124 contact **Ile 104, Leu 105, Leu 116, Cys 120, Val 123** and **Ile 127** of Skp1 (Schulman *et al.* 2000). Multiple sequence alignment has confirmed that these amino acids are conserved in *M. oryzae* as well.

Efforts were made to predict post translational modifications, like glycosylation, myristoylation etc. MoSKP1 lack a secretory signal peptide and is therefore unlikely to be exposed to the modifications like o-glycosylation. Although it has one Threonine site, the value (0.571) is very small, just above the threshold (0.5) value. No other secondary modification like DNA binding motif, Fatty acid acylation, Sulphonation site was predicted in this protein.

a



b



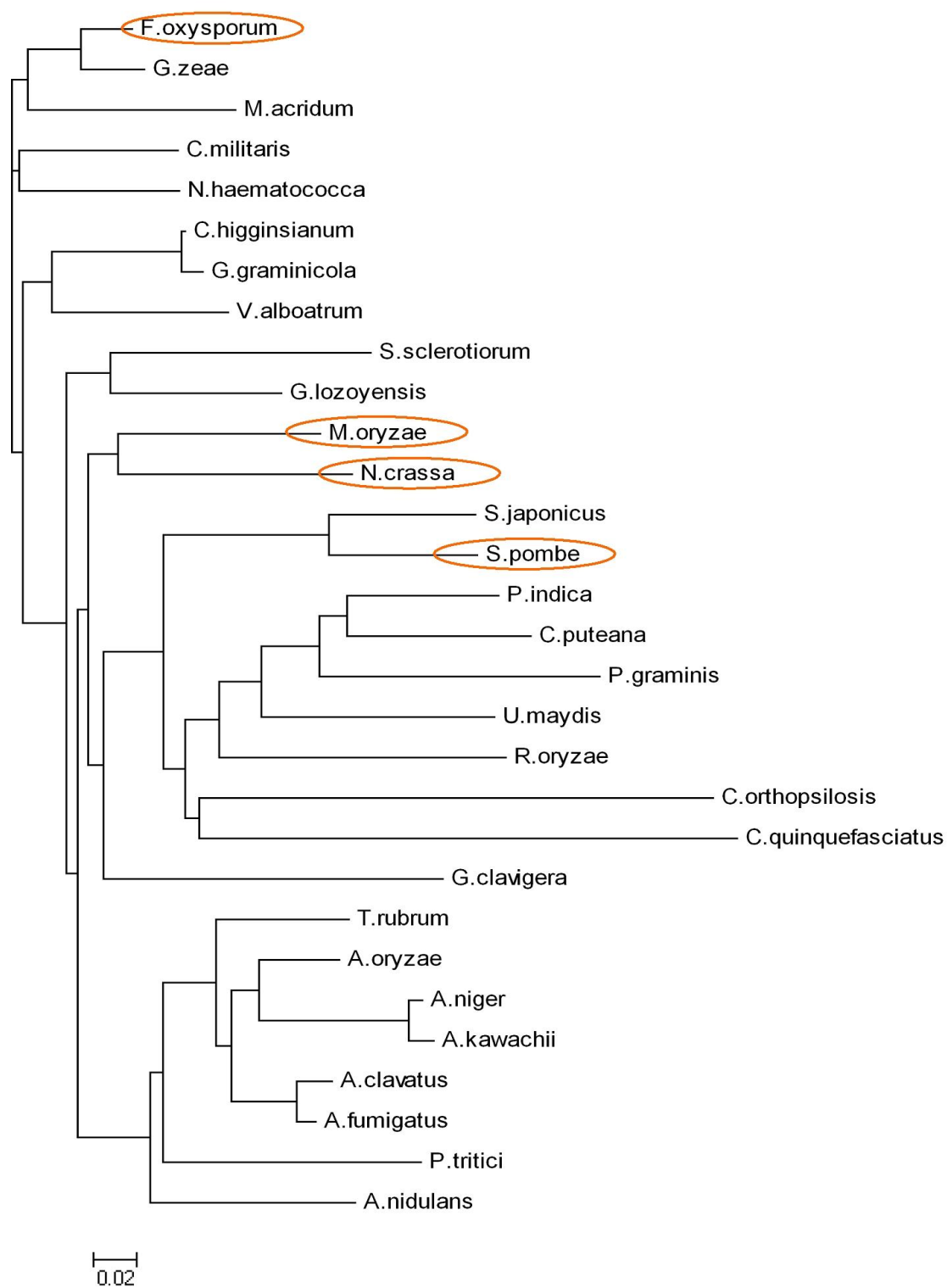


Figure 7: (a) Multiple sequences alignment using *M. oryzae*, *F. oxysporum*, *S. pombe*, Human and *S. cerevisiae* Skp1 protein sequences. Red arrow shows the conserved amino acids involved in F-box binding. Black trapezium shows site of phosphorylation predicted by NetPhos 2.0 software. **(b)** Sequence homology based domain prediction of *MoSkp1*

Figure 8: Dendrogram generated using 30 sequences which show up to 60 % identity at protein level. Circle shows *M. oryzae* is closest to *N. crassa* whereas *S. pombe* is closer to *M. oryzae* compared to *F. oxysporum*.

List of strains used in the development of phylogenetic tree. Phylogenetic analysis of *Magnaporthe oryzae* (XP_359799.1), *Fusarium oxysporum* (AAT85970.1), *Neurospora crassa* (XP_959019.1), *Verticillium albo atrum* (XP_003003165.1), *Gibberella zeae* (XP_387098.1), *Cordyceps militaris* (EGX94398.1), *Colletotrichum higginsianum* (CCF32791.1), *Nectria haematococca* (XP_003052201.1), *Glarea lozoyensis* (EHL00027.1), *Glomerella graminicola* (EFQ24879.1), *Metarhizium acridum* (EFY90756.1), *Trichophyton rubrum* (XP_003230905.1), *Grosmannia clavigera* (EFW98759.1), *Pyrenophora tritici* (XP_001931415.1), *Rhizopus oryzae* (EIE77840.1), *Aspergillus oryzae* (XP_001817076.1), *Aspergillus clavatus* (XP_001273939.1), *Aspergillus kawachii* (GAA89882.1), *Aspergillus nidulans* (XP_659906.1), *Aspergillus fumigatus* (XP_754026.1), *Aspergillus niger* (EHA22420.1), *Schizosaccharomyces japonicus* (XP_002174379.1), *Ustilago maydis* (XP_760758.1), *Puccinia graminis* (XP_003335788.1), *Sclerotinia sclerotiorum* (XP_001598454.1), *Coniophora puteana* (EIW84951.1), *Piriformospora indica* (CCA69667.1), *Culex quinquefasciatus* (XP_001843442.1), *Candida orthopsilosis* (CCG21169.1), *Schizosaccharomyces pombe* (NP_595455.1).

3.2 Cloning of *MoSkp1* and generation of anti-sense construct

On the basis of sequence information available from Broadmit, specific primers for *M. oryzae MoSKP1* were designed to amplify the gene of interest. First, primers were used to amplify a 3.645 kb fragment containing gene of interest. In this 3.645 kb fragment *MoSKP1* is flanked by ~1.5kb upstream and ~1.5kb downstream sequences. The forward and reverse primers used for amplification were: Forward primer: 5' TTGCCTCTGTGAACAGGGCAGAA 3' and Reverse primer: 5' AACGGACTGACTTTGTAAAGG 3'. The PCR program used was as follows: Initial denaturation at 94°C for 5min, denaturation at 94°C for 30 sec, annealing at 58°C for 30 sec, elongation at 72°C for 2 min; this cycle was run 29 times and final extension was given at 72°C for 5 min. A proof reading Taq polymerase enzyme (XT-5, Bangalore genei) was used. To check the amplification size of the PCR product 0.8% agarose gel was run along with 1 kb DNA marker. A 3.5 kb band was observed corresponding to 3466 bp DNA fragment amplification.

A blunt end ligation was carried out and 3466 bp PCR product was cloned in a cloning vector plasmid Bluescript KS + (pBSKS+). First the KS vector was digested with *EcoRV* enzyme (a blunt end generating enzyme) and gel purified. The purified PCR product was mixed with vector and ligation reaction was kept at 16°C for 4 h. *E. coli* DH5 α cells were transformed using this ligation mixture and colonies were selected on Luria Agar (LA) plate containing ampicillin to a final concentration of 100 μ g/ml. Clones were confirmed by restriction digestion with *XhoI* and *XbaI* (Fig. 9). In order to investigate the function of *MoSKP1* in *M. oryzae* B157, an antisense construct was generated by cloning the *MoSKP1* gene fragment in to a silencing vector, pSilent. This silencing vector has a TrpC

promoter and TrpC terminator with multiple cloning sites. The PCR product was digested with *XhoI* and *BglIII* along with vector and directional cloning was done. The DNA fragment is supposed to be in opposite orientation such that after transcription by TrpC promoter the mRNA will be complementary to the native *MoSkp1* mRNA. Then the antisense cassette (containing TrpC promoter, DNA fragment and TrpC terminator) was released by digesting with *XbaI* and mobilised into the vector pCAMgfp at *XbaI*. pCAMgfp is a binary vector which can be propagated in *E. coli* DH5 α as well as in the fungus. *Agrobacterium tumefaciens* mediated fungal transformation has the advantage over protoplast transformation that it gives predominantly single site insertion in the genome.

The *MoSkp1* antisense construct in pSilent was confirmed by digesting it with *EcoRI* enzyme. This gave 5 kb, 2.5 kb and 1.5 kb fragment, which confirmed that a ~2kb fragment was inserted into the vector. Then final antisense construct in pCAMgfp was also confirmed by restriction digestion using *XbaI* to release the cloned fragment from pSilent and a 4 kb fragment was observed confirming the construct (Fig.10 a&b).

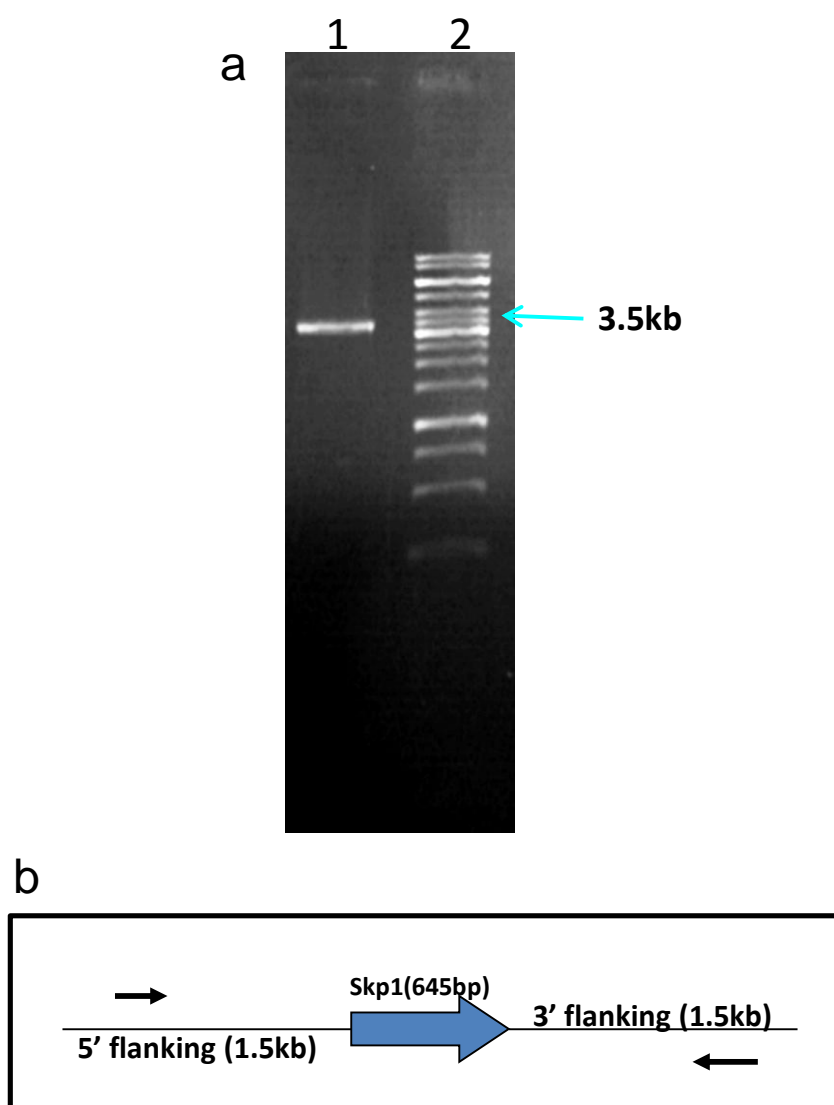


Figure 9: PCR product using gene specific primers and template from B157 genomic DNA for *MoSKP1* was run on 0.8% Agarose gel

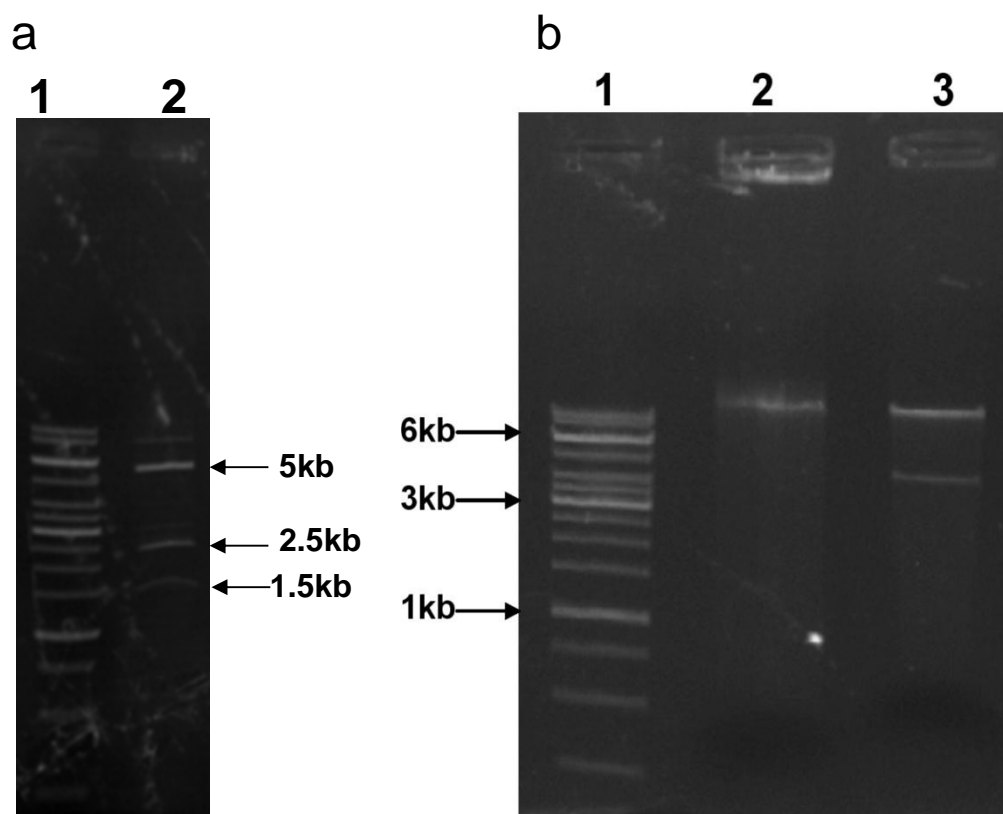


Figure 10: (a) Confirmation of pSILENT-MoSkp1 antisense construct by restriction digestion with *EcoRI*. Lane 1 has 1kb DNA ladder and Lane 2 has *EcoRI* digested construct showing release of band which confirms the construct. (b) Confirmation of antisense pCAMgfp-Skp1 construct digested with *XbaI* which gives a release of 4 kb

3.3 Mobilisation of antisense construct in *Agrobacterium* by Triparental mating

The *MoSKP1* antisense construct generated was then mobilised into *A. tumefaciens* LBA4404 strain by triparental mating. The above antisense construct was used for fungal transformation by *A. tumefaciens* mediated transformation. After mobilising in *Agrobacterium*, the presence of the construct was confirmed by restriction digestion. The *Agrobacterium* was further checked by keto-lactose test. Three separate colonies were screened for the presence of *MoSKP1* antisense construct (Fig. 11a).

3.4 Fungal transformation by ATMT

Fungal transformation of *M. oryzae* B157 with *MoSKP1* antisense construct was performed by the ATMT method. Transformation was done with 1×10^5 spores per ml of solution. *A. tumefaciens* containing antisense construct (pCAM-Skp1) was grown in AB liquid media and induced with Acetosyringone (200 μ M final concentration) for 6 h at 28°C. Infection was allowed at room temperature and selection of putative transformants was done on complete media containing Hygromycin to a final concentration of 200 μ g/ml and Cefotaxime up to 200 μ g/ml. After three successive transformation ~100 putative *MoSKP1* antisense transformants were screened (Fig. 11b). These putative MoSkp1 antisense transformants were further analysed and 26 transformants were selected for phenotypic characterisation.

3.5 Phenotypic characterization of putative antisense fungal transformants

Approximately 100 putative *MoSKP1* antisense transformants which were growing on Hygromycin B plate were analysed for pathogenicity related characters like growth, melanin production, sporulation and appressoria formation. The transformants showing

positive results were selected for further analysis. *SKP1* is known to be involved in the cell cycle progression in *S. pombe* and kinetochore assembly in *S. cerevisiae*. In *S. pombe* SCF is necessary to cross G2/M checkpoint in cell cycle. Skp1 is an integral part of SCF E3 ubiquitin ligase and in the absence of SCF, DNA damage checkpoint gets activated and thus cells remain in G2 phase. In the *S. pombe* mutant (Skp1A7 *S. pombe*) it has been shown that G2 delay gives an elongated phenotype of the cell, where cells continue to grow but are unable to divide. Based on this information, transformants showing reduced growth, less sporulation, appressorial defects were selected. It is also known that mitosis is necessary for the development of appressoria (Table 1). Out of 100 putative antisense transformants, 26 transformants showed delay in growth which leads to less sporulation. Of these, 4 transformants were affected in appressorial development also. These four transformants which showed retarded growth, less sporulation and no appressoria formation were selected for further analysis. These transformants were unable to form appressoria even after 36 h when incubated at 28°C and 90% humidity (Fig. 12). Equal size of mycelia plugs were kept on plate and the growth was measured as the diameter of the growing culture after 4th and 5th day. For sporulation assay, spores were extracted in equal volume of water and counted in a Neubauer chamber under a microscope. Some other phenotypes were observed in these transformants like late development of germ tube (A1 and A6) and more than one germ tube from single conidia (A4 and A15.1). The sporulation assay indicates that sporulation in these transformants was reduced to 50% as compared with the wild type *M. oryzae* B157 strain.

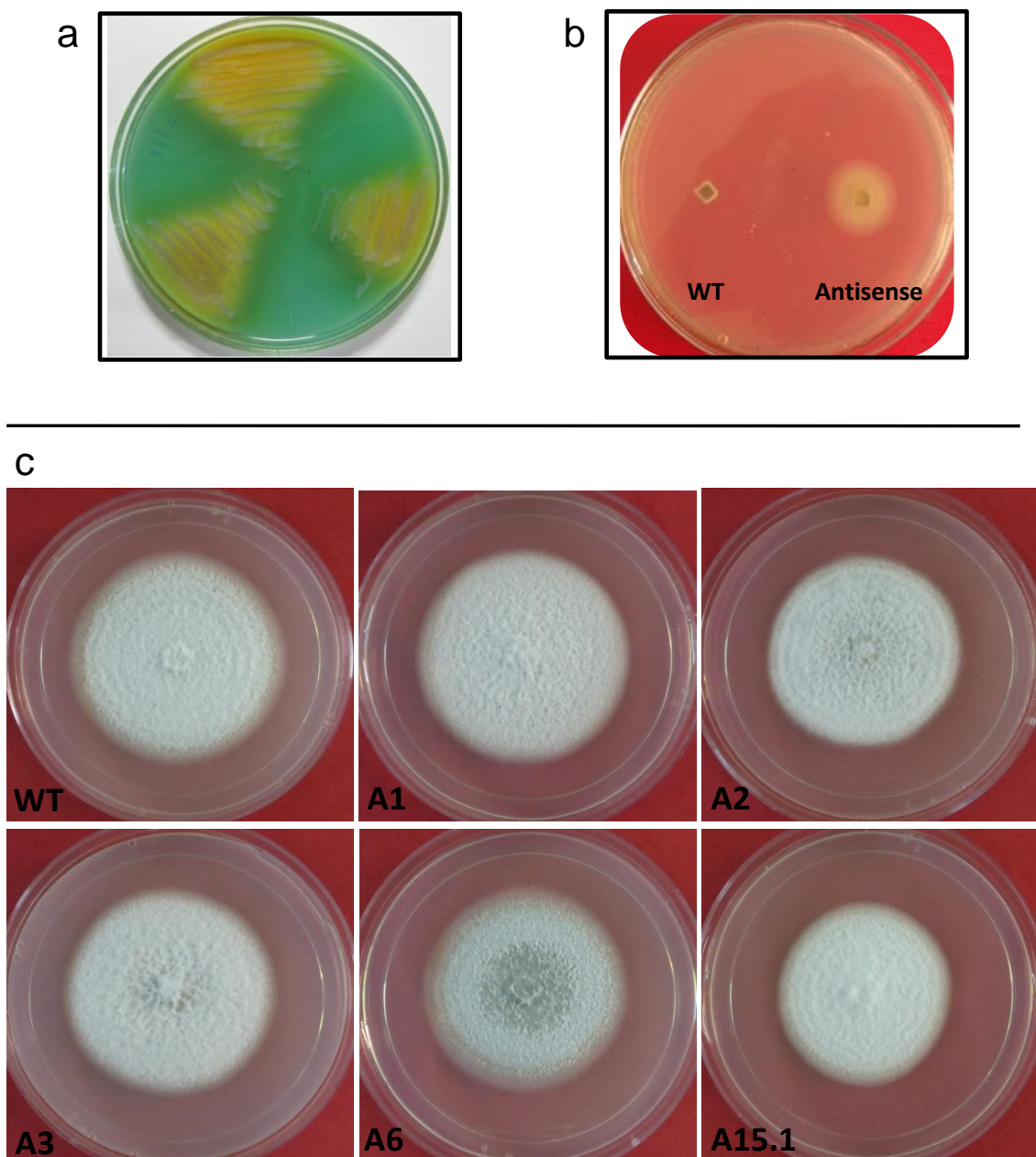


Figure 11: (a) *Agrobacterium tumefaciens* LBA4404 containing antisense construct overlaid by Benedict Reagent showing yellow halo around streaked culture. (b) Photographs of MoSKP1 antisense transformants selected on complete minimal (CM) agar media plate containing Hygromycin B (200µg/ml) after 3 days. (c) Morphology of MoSKP1 antisense transformants on OMA plate

Table 1.

SN	Tra	Growth Assay(mm)				Sporulation($\times 10^4$ /ml)				Appressoria(out of 100)			
		1	2	3	Av	1	2	3	Av	1	2	3	Av
1	WT	20	22	21	21	200	220	190	203	80	85	86	84
2	A1	5	5	6	5.3	50	45	55	50	40	45	39	41
3	A2	17	18	16	17	150	175	190	171	75	80	79	78
4	A3	16	15	14	15	176	180	200	185	90	80	78	83
5	A4	6	4	6	5.3	180	190	210	193	30	40	41	37
6	A5	18	19	20	19	190	200	180	190	85	90	88	88
7	A6	7	8	5	6.6	47	35	45	42	28	30	36	31
8	A7	19	20	17	18.6	210	210	190	203	76	80	85	80
9	A8	17	19	21	19	230	200	240	223	75	80	79	78
10	A9	18	21	20	19.6	190	200	210	200	80	90	81	84
11	A10	17	18	19	18	180	200	180	187	70	75	79	75
12	A11	19	16	17	17.3	175	190	200	188	80	85	89	85
13	A12	20	17	19	18.6	195	220	190	202	76	80	75	77
14	A13	21	20	21	20.6	185	230	210	208	80	79	78	79
15	A14	22	22	23	22.3	175	200	175	183	70	80	76	75
16	A15.1	7	8	9	8	60	45	54	53	25	30	32	29
17	A16	18	20	21	19.6	210	200	230	213	85	82	80	82
18	A17	19	21	20	20	200	210	235	215	90	85	86	87
19	A18	20	23	25	22.6	189	230	200	206	75	80	82	79
20	A19	21	21	23	21.6	150	190	210	183	90	86	88	88
21	A20	17	19	23	19.6	140	175	180	165	80	90	85	85
22	A21	18	20	21	19.6	180	200	190	190	85	78	79	81
23	A22	20	24	25	23	175	200	200	192	85	80	75	80
24	A23	23	24	25	24	165	180	189	178	70	75	79	75
25	A24	23	21	19	21	190	210	230	210	80	82	88	83
26	A25	18	20	21	19.6	220	230	240	230	80	85	86	84

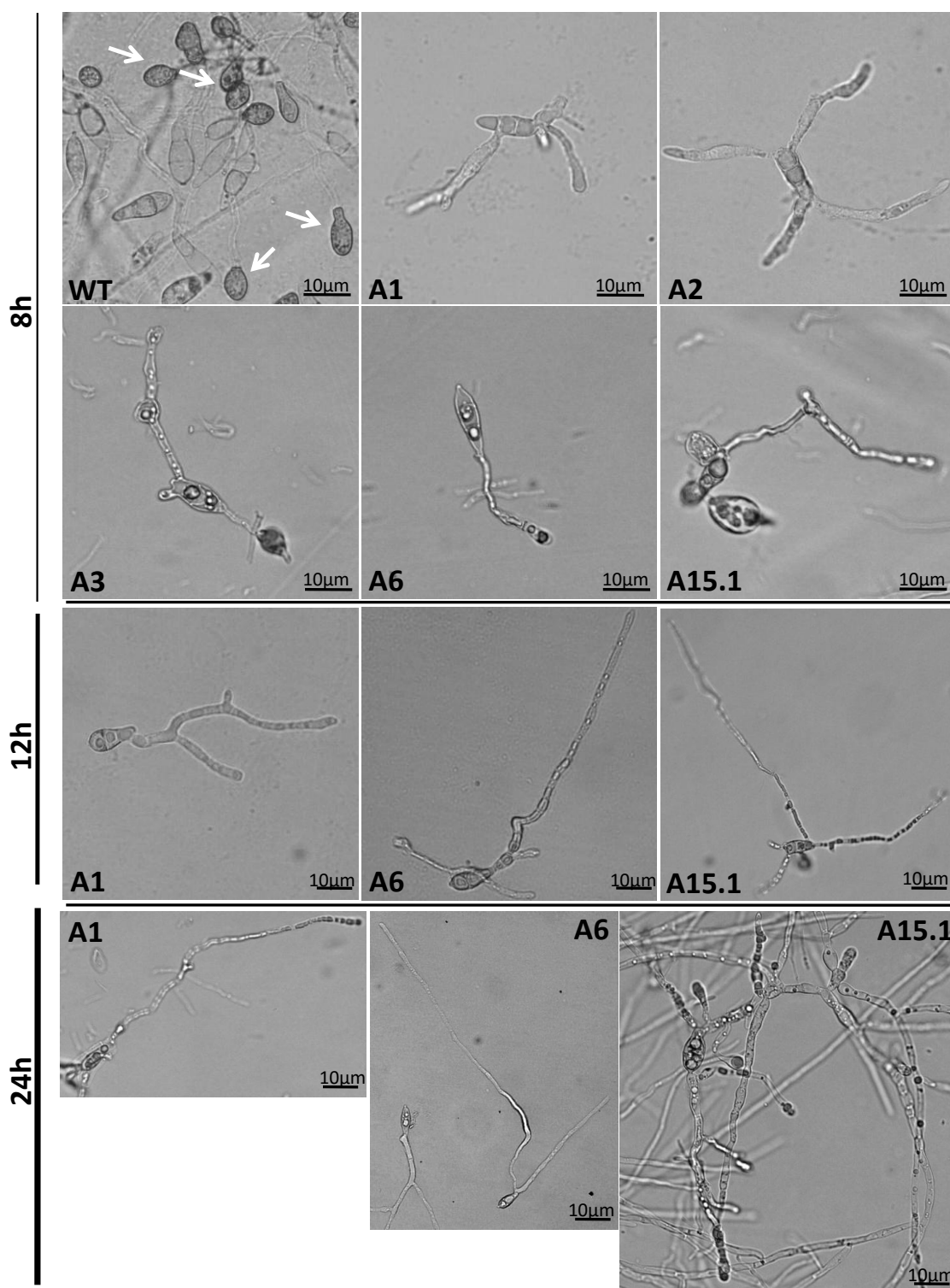


Table 1: Growth, sporulation and appressorial assays were performed for *MoSKPI* antisense transformants. Transformants in bold showed reduction in growth, sporulation and appressoria development.

Figure 12: Appressorial assay of *MoSKPI* antisense transformants compared with the wild type B157 at 8h, 12h and 24h of incubation at 28°C and 90% humidity on hydrophobic slides

3.6 A dual selection based targeted gene replacement tool in *Magnaporthe oryzae* and development of *MoSKP1* disruption vector

A dual selection based, targeted gene replacement tool has been devised for *Magnaporthe oryzae* (Khang et.al. 2005) using pGKO1 vector. This method is based on ATMT with a mutant allele of the target gene flanked by the herpes simplex virus thymidine kinase (*HSVtk*) gene as a conditional negative selection marker against ectopic transformants. The *HSVtk* gene product converts 5- fluoro-2'-deoxyuridine (F2dU) to a compound toxic to diverse fungi. pGKO2 is another derivative of pGKO1 vector, where *HSVtk* gene is placed before the MCS. The pGKO2 vector was used in this study. KS-*Skp1* clone was first digested with *Xho* I and *Xba* I to release 2.5 kb fragment which was finally cloned in to a dual selection vector pGKO2 at *Xho* I/ *Xba* I sites. This clone was confirmed by restriction digestion with *Xho* I and *Xba* I enzymes (Fig. 13a). The pGKO2-*Skp1* vector was digested with *Sal* I which cuts in the middle of the gene and a 1.4 kb hygromycin phosphotransferase (*hpt*) taken from pCAMgfp vector by digestion with *Sal* I was then sub cloned at *Sal* I site of pGKO2-*Skp1* vector by means of sticky end ligation. This construct was then confirmed by restriction digestion with *Sal* I enzyme to release a 1.5 kb band (Fig. 13b).

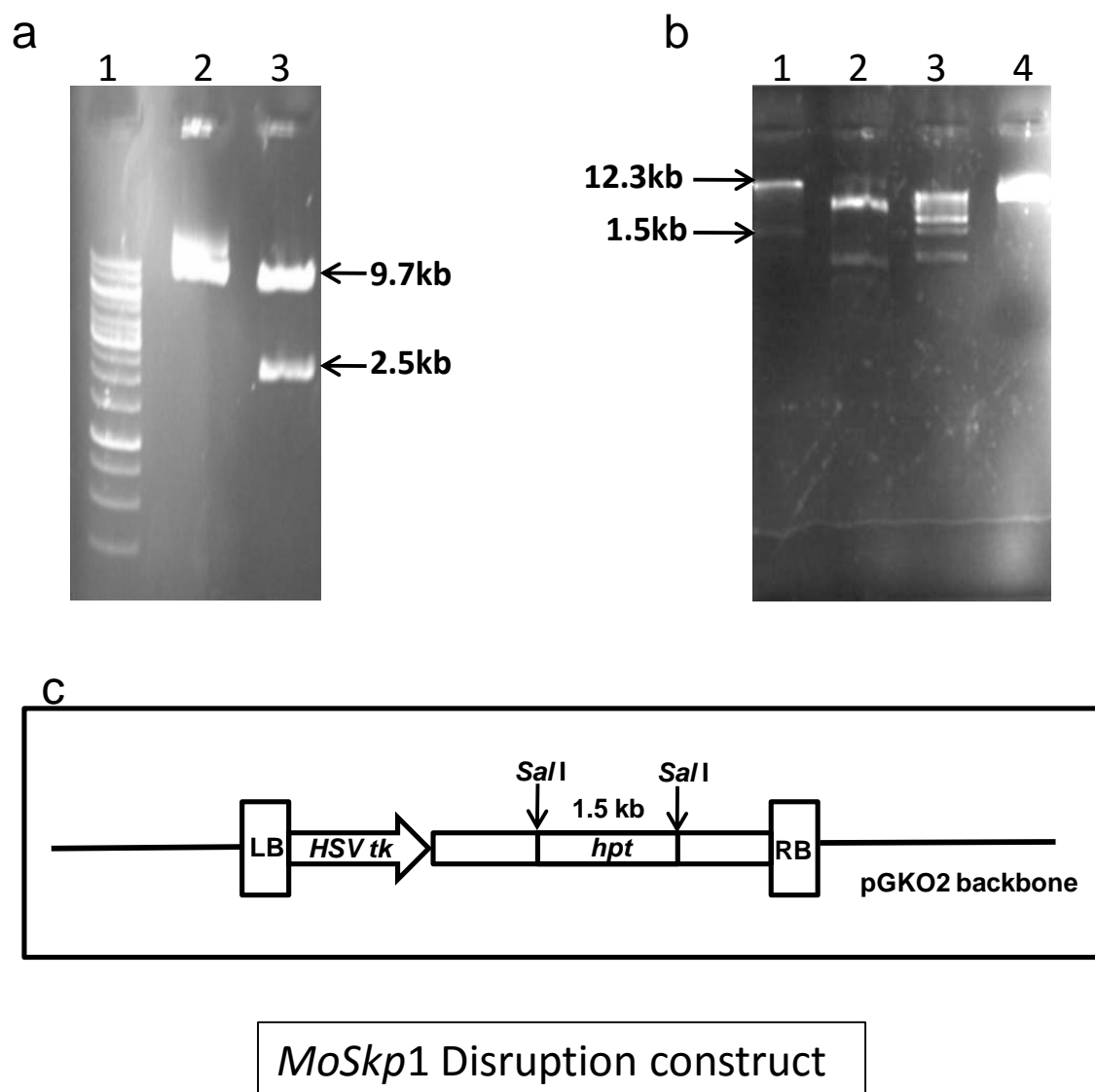


Figure 13: (a) Confirmation of sub-cloning of *MoSKP1* fragment into dual selection vector pGKO2 by restriction digestion. Lane 1 - 1kb DNA molecular marker, lane 2 - undigested plasmid and lane 3 - digested plasmid with *XhoI* and *XbaI* showing release of 2.5 kb band. (b) Disruption of *MoSKP1* gene by inserting *hpt* cassette in *MoSkp1*-pGKO2 constructs. Construct was confirmed by digesting with *SalI* enzyme. Lane 1 - construct digested with *SalI*, lane 2 - construct digested with *XhoI* and *XbaI*, lane 3 - 1kb DNA molecular marker, lane 4 - undigested construct. (c) Pictorial representation of *MoSKP1* disruption cassette in pGOK2 vector

3.7 Transformation of *M. oryzae* B157 strain using *MoSKPI* Disruption constructs

An effort was made to transform *Magnaporthe* B157 strain by ATMT approach using *MoSKPI* disruption construct. Disruption construct was mobilised to *Agrobacterium* by triparental mating and then fungal transformation was done. The frequency of putative transformants was found to be very low. Only 25 transformants were recovered from one transformation. These transformants were checked for the integration by PCR and we obtain native gene amplification along with disrupted gene. This observation indicates that integration was ectopic. In two more successive transformations, similar results were observed and we were unable to isolate a transformant with true disruption of the *MoSKPI* gene.

3.8 Development of RNAi and overexpression construct for *MoSKPI*

RNAi mechanism is well established and studied in *M. oryzae* system. For the development of *MoSKPI* RNAi construct another silencing vector was used, which is known as pSilent Dual (pSD2). This vector has two promoters (TrpC promoter) for transcription in opposite directions flanking the multiple cloning site (MCS). Thus, once a fragment of DNA is cloned in MCS of this vector, it will be divergently transcribed from both side strands and forms double stranded RNA. Double stranded RNA cannot be present in cells as such and gets digested into small fragment of 21 nucleotides. These 21 nucleotide RNAs lead to initiation of RNAi machinery in cell. For generation of *MoSKPI* RNAi construct, a 645bp *MoSKPI* ORF was amplified using specific primers and cloned in pSD2 vector at *Hind* III and *Xho* I site. This construct was confirmed by restriction digestion with the same enzyme to release the cloned fragment (Fig. 14). Similarly,

overexpression construct was generated by cloning the PCR product in pSilent vector at *Kpn* I and *Hind* III site in right orientation. The clone was confirmed by restriction digestion.

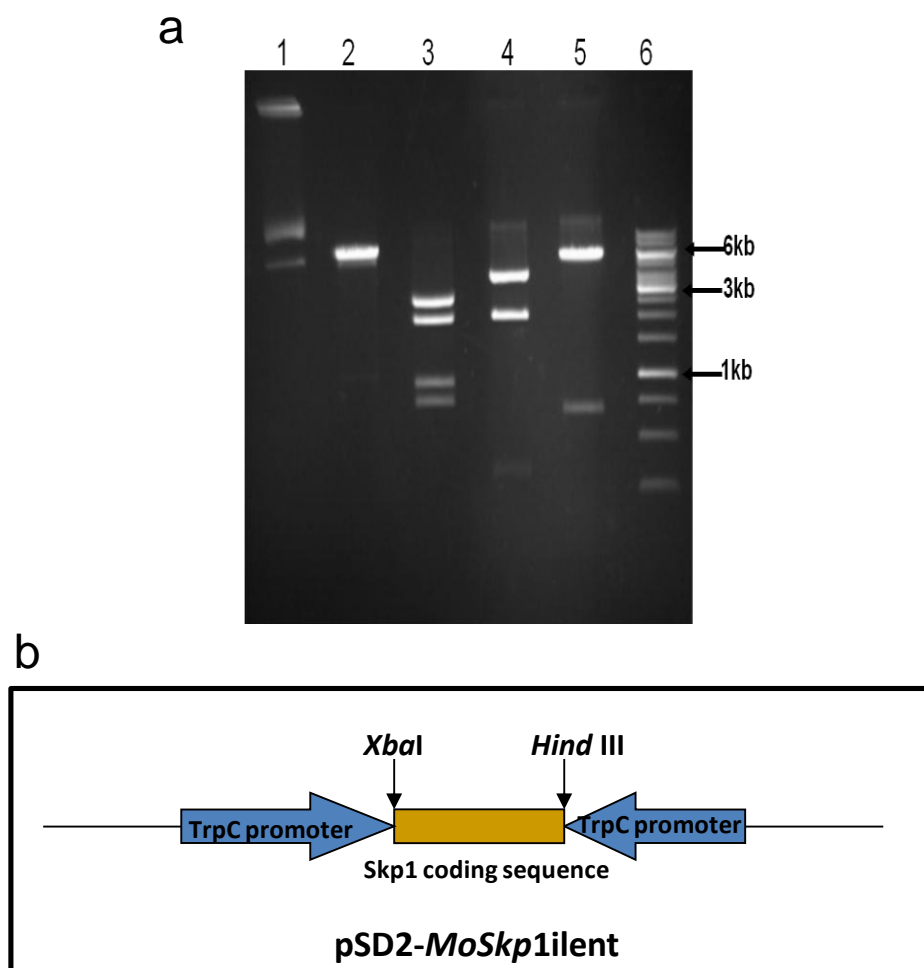


Figure 14: (a) Confirmation of *MoSkp1*-pSD2 RNAi constructs. Lane 1 - undigested plasmid, lane 2 - *EcoRV* digest, lane 3 - *PvuII* digest, lane 4 - *PstI* digest, lane 5 - *XhoI* and *HindIII* digest of construct, lane 6 - 1kb DNA ladder. (b) Pictorial representation of *MoSkp1*-pSD2 RNAi construct

3.9 Protoplast transformation of B157 strain using *MoSKPI* RNAi and overexpression constructs

Conditions for protoplast transformation were optimised using *MoSKPI* RNAi construct and overexpression construct. This construct does not have any T-DNA border so ATMT cannot be utilised for transformation. A good efficiency of transformation was found for the RNAi construct. In this transformation 1×10^6 protoplasts cells were used with $5 \mu\text{g}$ of plasmid DNA and 25 putative RNAi transformants were recovered. These putative transformants were primarily screened for the transfer of transgene by PCR and integration of gene was confirmed by Southern hybridization.

3.10 Screening of putative RNAi and overexpression transformant of *MoSKPI*

The primary screening of *MoSKPI* RNAi transformants was done by checking the ability of the transformants to grow on Hygromycin supplemented YEG agar plate. 25 putative transformants growing on the selection plates were further screened by PCR. Specific primers were designed against the selection marker Hygromycin phosphotransferase (*hpt*) gene and presence of the transgene was confirmed by amplifying in the RNAi transformants. The PCR conditions were optimised and the following primer set, Hpt For - 5'AGGGCGAAGAATCTCGTGCTTTC3' and Hpt Rev- 5'CCACTATGGGCGAGTACTTCTAC3' were used for screening. A 990bp amplification was observed corresponding to the gene length of *hpt*. These transformants were further used for phenotypic characterisation and genomic integration was confirmed by Southern blot analysis (Fig. 15 a&b). Similarly, *MoSKPI* over expression

transformants were also screened and two transformants were used further for phenotypic and molecular characterisation.

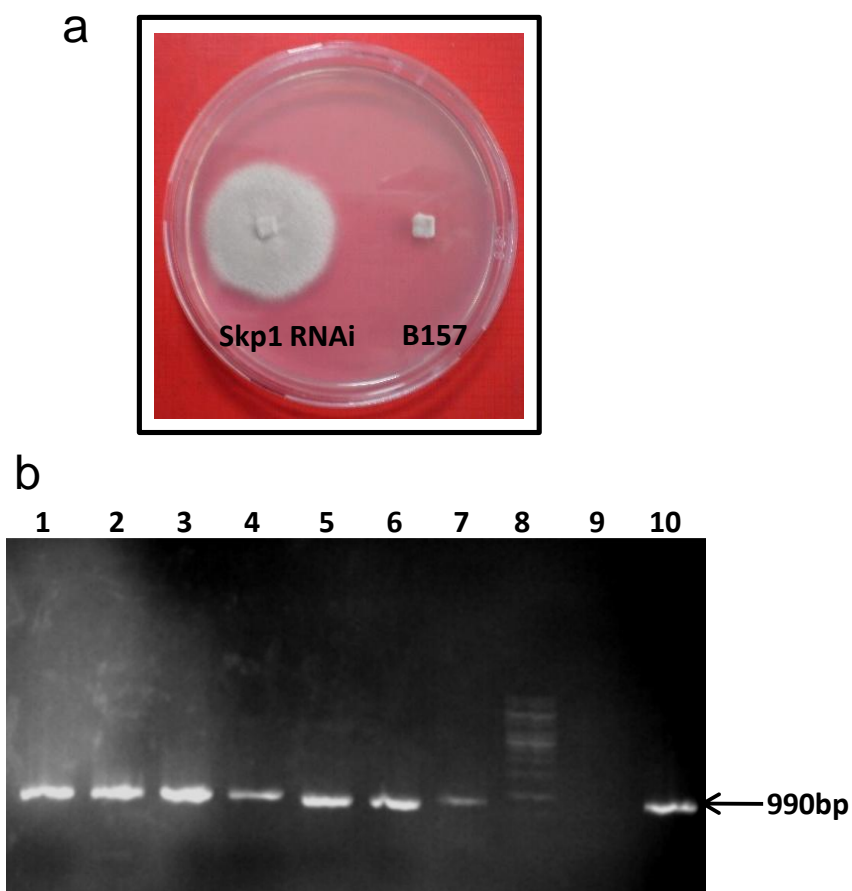


Figure 15: (a) *MoSKPI* RNAi transformants were selected on CM agar containing Hygromycin B (200 µg/ml) plate. (b) PCR screening of putative *MoSKPI* RNAi transformants using *hpt* specific primer. Amplification of 990 bp was observed in transformants whereas there was no amplification was seen in wild type *M. oryzae* B157 strain

3.11 Interspecies gene complementation study of *MoSKP1*

Bioinformatics analysis showed that *MoSKP1* was close to *S. pombe Skp1*. *S. pombe* (Fission yeast) is a good model system to study cell cycle events and for complementation studies. A temperature sensitive mutant of *skp1* in *S. pombe* (*skp1A7*) was provided by Prof. Takashi Toda (Laboratory of Cell Regulation, Cancer Research, UK). *skp1A7* mutant of fission yeast shows G2 delay, elongated cell phenotype, defects in chromosome separation and in septum. Yeast expression vector was generated by cloning cDNA of *MoSKP1* into pYES2 vector at *XhoI* and *XbaI* sites. *skp1 A7* yeast transformation was performed by lithium acetate method using pYES2-MoSkp1 construct. Plasmid YES2 contains an inducible GAL1 promoter and URA3 gene as selection marker. The clone was confirmed by restriction digestion and named pYES2-MoSkp1. Transformants were selected on EMM (Edinburgh Minimal Media) without uracil. Another *skp1A7* yeast transformation was done with empty vector (pYES2) and the phenotype of transformant was checked. Wild type *S. pombe*, *skp1 A7* mutant and complemented *skp1 A7* containing pYES2-MoSkp1 vector, were grown under induced conditions (in presence of Galactose as sole Carbon source) at restrictive temperature and the length of the cells were measured under microscope (Olympus BX51) at 40x magnification and picture was taken in oil immersion 100x objective lens. The normal size of wild type fission yeast was found to be ~10 μm whereas *skp1 A7* mutant were up to ~18 μm . Cell length returned to normal size in complemented strain Skp1 A7- pYES2-MoSkp1. 200 cells were independently counted for wild type, mutant and complemented strains of *S. pombe* and length was measured for each cell. A graph was generated to show the average length of all the strains at restrictive temperature (Fig. 16).

3.12 Nuclear staining of complemented Fission yeast

Nuclear staining was done to localise nucleus of the fission yeast cell and to demonstrate the nuclear organisation in cell division. All cells, wild type, mutant *skp1 A7*, and complemented strain Skp1 A7-pYES2-MoSkp1 were grown under induced condition (in presence of 2% w/v Galactose as sole source of Carbon) at the restrictive temperature of 37°C. Cells were washed and fixed on the slide. For staining the nucleus, Hoechst stain was used and the cells were observed under fluorescent microscope (BX51 Olympus) with 100x magnification. *skp1 A7* mutant has diffused nucleus (Fig. 17a) indicating that cells are in active phase but the cell growth is continuing and so cell getting elongated. When MoSkp1 is expressed in this mutant, cells were able to divide; the nucleus showed normal organisation and cell size became normal.

3.13 Cell septum staining of complemented Fission yeast

In order to study cytokinesis of complemented strain of fission yeast Skp1-pYES2-MoSkp1, cell septum was stained. After CFW staining, defective division of *skp1 A7* mutant was rescued in complemented fission yeast strain Skp1-pYES2-MoSkp1 (Fig. 17b). It has been shown in fission yeast that Skp1 is involved in coordinated structural alteration in mitotic spindles and nuclear membranes (Lehman et al. 2004), so it can be predicted from complementation experiment, that in *M. oryzae* Skp1 is coordinating the chromosome segregation and in absence of MoSkp1, cells are unable to divide because of which MoSkp1 RNAi and antisense transformants were showing slow growth, less sporulation and were unable to form appressoria.

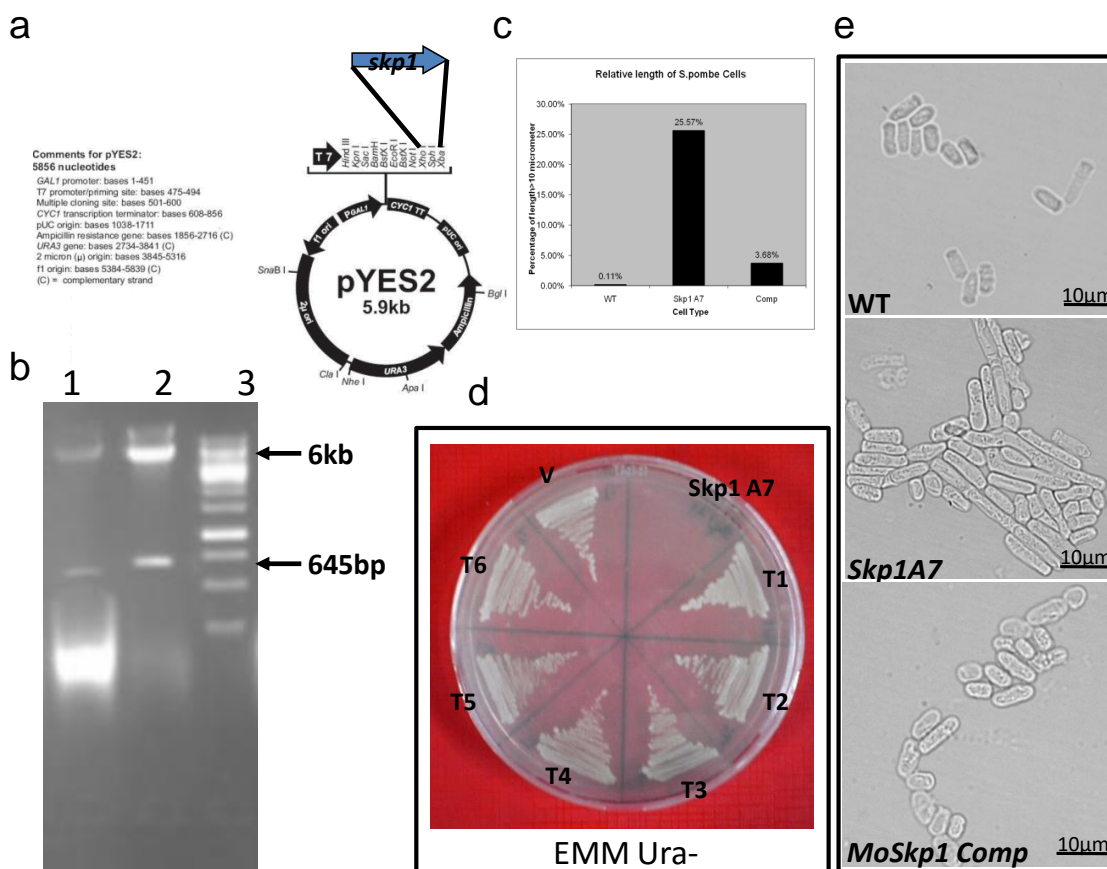


Figure 16: (a & b) pYES2-*MoSkp1* construct confirmation was done by release of a 645 bp cloned fragment of *MoSKP1* with enzyme *XhoI* and *XbaI*. Lane 1 and 2 contains product of pYES2-*MoSkp1* digested with both enzymes and lane 3 contains 1 kb DNA ladder. Phenotypic study of complemented *skp1 A7* mutant. (c) *S. pombe skp1 A7* strain was transformed with pYES2-*MoSkp1* expression vector and pYES2 empty vector and selected on EMM agar without Uracil. (d) Cells were grown at 25°C and then transferred to 37°C for 4 h and length of *S. pombe MoSKP1* transformed cells and *skp1 A7* mutant was observed under microscope. For each strain 100 cells were counted and percentage of cells with elongated phenotype was calculated. Experiment was done in triplicate and level of significance was calculated at 5% P-value. (e) Micrograph of wild type, *skp1 A7* mutant and the complemented strain was observed at 100x magnification

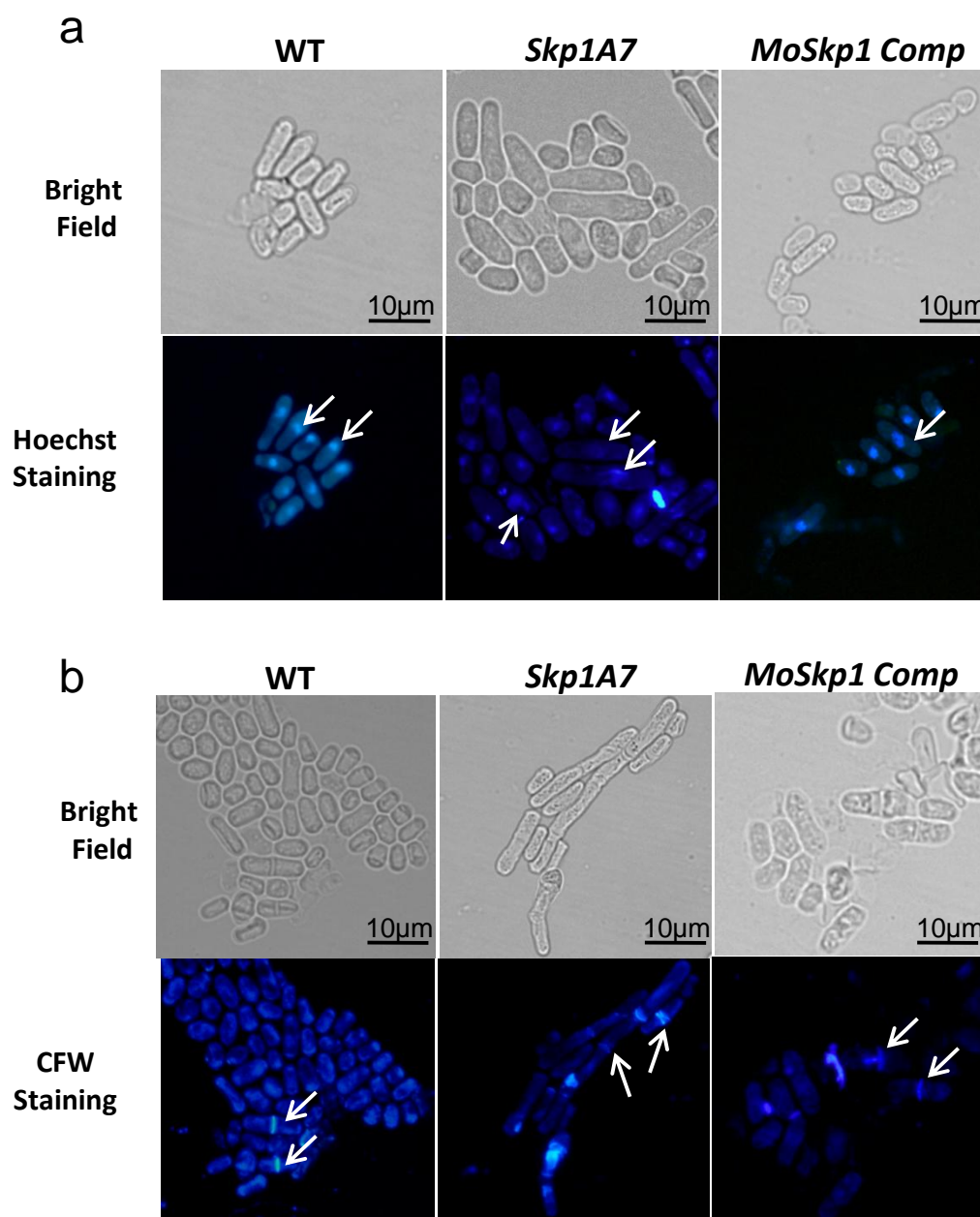


Figure 17: (a) Nuclear staining was done using Hoechst 3342 stain to visualise the nuclear organisation. Cells were grown in EMM broth at 25°C and transferred to 37°C for 4 h, 50 μl of cell suspension was fixed and stained with Hoechst 3342 stain for 10 min and observed by using fluorescence microscopy. (b) Septum of *S. pombe* was stained with Calcofluor White stain. Cells were induced at restrictive temperature. Around 200 cells were counted for each strain and percentage of multi-septate cells was determined

3.14 Heterologous expression of *MoSKP1*, purification of MoSkp1 protein and antibody generation

In order to express *M. oryzae* Skp1 protein a heterologous protein expression system was developed. Initially an attempt was made to develop yeast expression system and the gene of interest (*MoSKP1*) was cloned in pPICZ α C vector, which is a *Pichia pastoris* expression vector with a signal sequence so that the expressed protein gets secreted in the cell supernatant. For unknown reasons, it was not possible to get good expression in that system and thus a bacterial expression system was used. Total RNA was isolated from *M. oryzae* B157 and cDNA of *MoSKP1* (501bp) was synthesised and cloned in pET30a, a bacterial expression system which has a 6xHis tag for affinity purification of protein. An induced band at 24 KD was observed on gel which corresponds to the expected size of protein MoSkp1 (Fig. 18). The recombinant MoSkp1 protein was purified by affinity chromatography using Ni-NTA column. The purified protein was further used for generation of polyclonal antibody in rabbit.

Generation of Polyclonal Antibody: In order to generate antibody against *M. oryzae* Skp1 protein white New Zealand rabbits were immunised with purified MoSkp1 protein. For the first dose 100 μ g purified protein was mixed with equal volume of complete Freund's Adjuvant and injected subcutaneously. 21 days after the first dose, two booster doses were given to the rabbit. Blood was withdrawn after one week after the second booster dose and serum was separated. Titer of the antibody was determined by the ELISA and western blot analysis was done to check the specificity of the antibody.

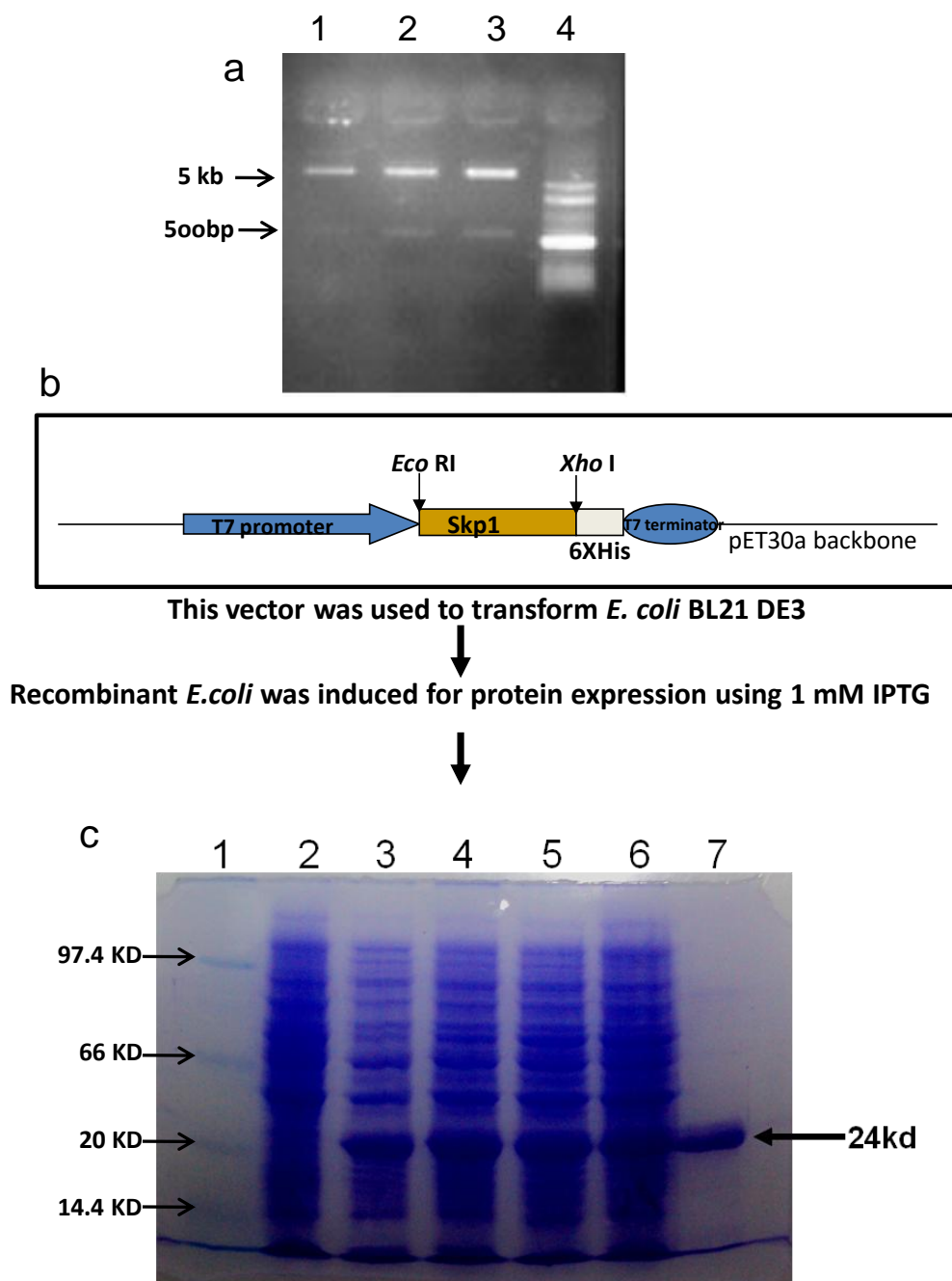


Figure 18: Confirmation of pET30a-*MoSkp1* construct and protein purification. **(a)** The clone was confirmed by restriction digestion with *Eco*RI and *Xho*I enzymes to release the cloned fragment of 500bp. **(b)** Pictorial representation of pET30a-*MoSkp1* construct. **(c)** The protein was expressed by inducing it with 1 mM IPTG for 4 h at 37°C and 200 rpm. 12% Polyacrylamide gel containing uninduced and induced protein sample along with purified protein was run

Molecular characterisation of antisense and RNAi transformants

3.15 Southern hybridisation analysis of antisense and RNAi transformant

To check the integration of the vector construct, Southern hybridisation was performed with *MoSKP1* RNAi and antisense transformants. For MoSkp1-RNAi transformants, five transformants were selected and genomic DNA was digested with *HindIII* enzyme, whereas for antisense MoSkp1, four transformants were selected and digested with *XbaI*. For probe preparation, a 350 bp fragment of TrpC promoter was amplified and labeled with chemifluorescent according to manufacturer's instructions (Amersham, USA). In case of RNAi transformants the enzyme cut in between the two TrpC promoters to yield one large fragment and a small fragment, and both fragments can be detected by using TrpC probe. Thus, for a single integration event two bands of different sizes are expected. In the case of antisense transformants the enzyme cuts at one side of probe and this results in a single band if there is a single integration event. The same probe was used for both blots. In RNAi transformants, two bands of different sizes were observed (Fig. 19 a&b). Bands also appeared at the top of the gel, which seems to be undigested DNA.

3.16 Detection of siRNA in RNAi transformants and antisense transformants

Small interfering RNA, a 21 nucleotide sequence, is the product of RNA silencing machinery. These siRNAs can readily be detected in transformants which confirms that RNAi mechanism is working in the system. In order to confirm RNAi-mediated silencing of the Skp1 gene in *MoSKP1* RNAi transformants and antisense transformant, siRNA was looked for in these transformants. Total RNA was isolated from the transformants

and wild type *M. oryzae* B157. The small RNA was enriched by polyethylene glycol (PEG 8000) and sodium chloride. The blot was hybridised with cDNA of *SKP1* as a probe. A specific primer was also run along with small RNA to compare the size of small RNA. Small interfering RNA of *SKP1* gene was detected in *MoSKP1* RNAi transformants (Fig. 20 a&b). Since it has been reported that antisense machinery finally leads to siRNA production, antisense transformants of *MoSKP1* were also used in this study and small RNA in antisense transformant was detected as well (Fire *et al.* 1998).

3.17 Quantitative analysis of *SKP1* transcript in antisense transformants and RNAi transformants

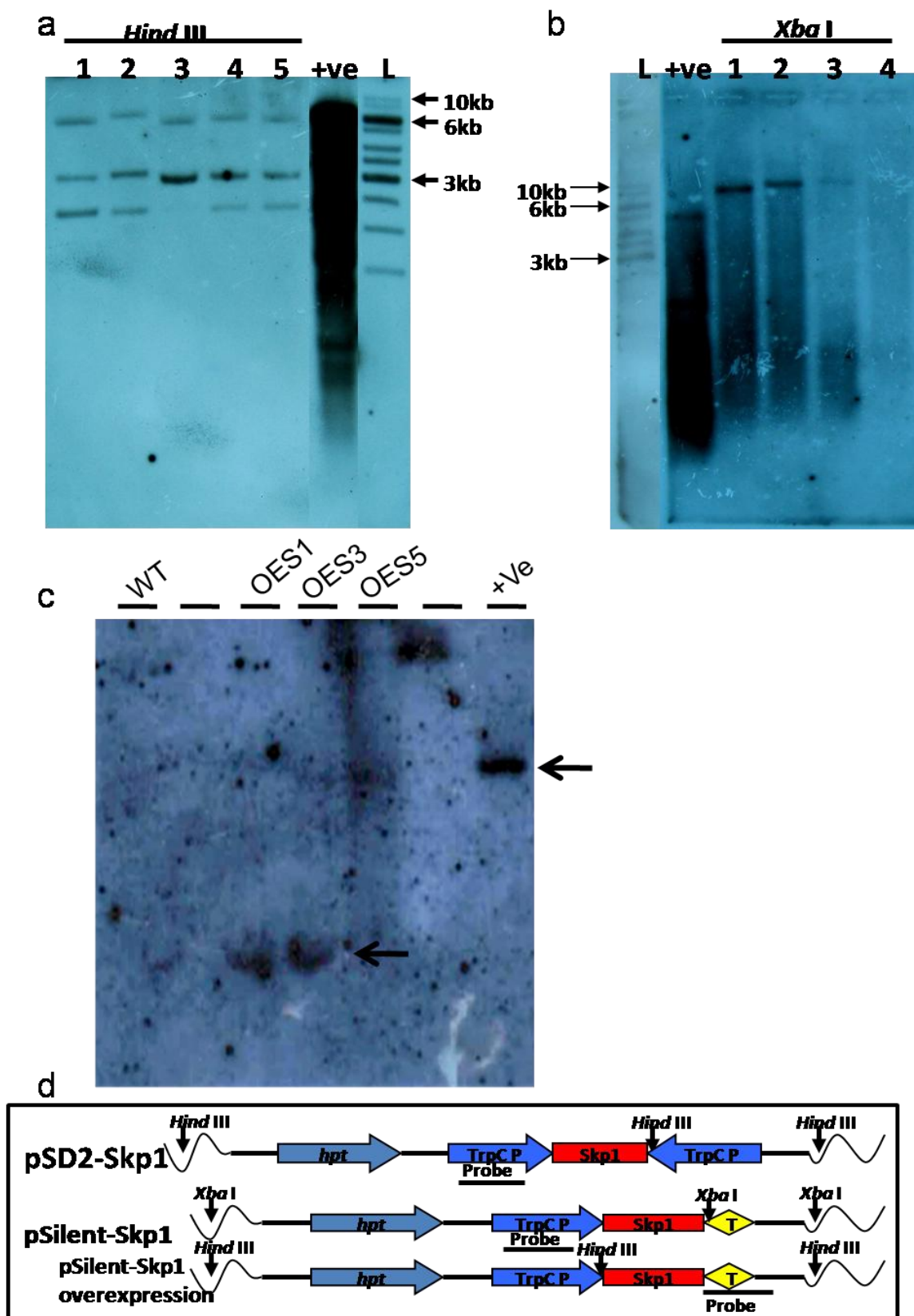
To check the intact *Skp1* transcript levels in knockdown transformants, a quantitative real time PCR was performed. The primers were designed so as to amplify 100bp from the C-terminal end of the mRNA to ensure the detection of the remaining *MoSKP1* mRNA. In this experiment, *β -tubulin* was taken as internal control. PCR conditions were optimised in terms of annealing temperature for both *SKP1* cDNA and *β -tubulin* gene. Fold change of target gene transcript was calculated by using formulae $2^{-\Delta\Delta Ct}$, where $\Delta\Delta Ct = (Ct_{\text{gene of interest}} - Ct_{\text{tubulin}})_{\text{test condition}} - (Ct_{\text{gene of interest}} - Ct_{\text{tubulin}})_{\text{control}}$, and relative abundance of target gene transcript was normalised to that of the *tubulin* gene for each RNAi transformants as $2^{-\Delta Ct}$ where $\Delta Ct = (Ct_{\text{gene of interest}} - Ct_{\text{tubulin}})$. Each RT-PCR quantification was carried out in triplicate and values for each gene were normalised to the expression level of the respective control condition and used further to calculate the ratio of the expression level of the requisite transcript. For *MoSkp1* RNAi transformants, five transformants were selected for real time PCR analysis showing upto 90% reduction of *MoSkp1* transcript

(Fig. 21a). The transcript levels of MoSkp1 antisense transformants were compared with wild type *M. oryzae* B157 and up to 70% reduction of transcript level was observed (Fig. 21b).

3.18 Ubiquitination enrichment assay of *MoSKP1* RNAi transformant

The ubiquitin proteasome pathway is the principal mechanism for protein catabolism. This pathway is significantly involved in regulating a variety of cellular processes including DNA repair, signal transduction, cell metabolism and growth (Oh *et al.*, 2012). Both differences in total ubiquitination and the ubiquitination of specific proteins affect numerous pathological conditions. Since the MoSkp1 protein stabilises E3 ubiquitin ligase, ubiquitination enrichment assay was carried out to see the ubiquitination profile in *M. oryzae* RNAi transformants. RNAi transformant R6 with 70% transcript reduction was selected and total ubiquitinated protein was enriched using an anti-ubiquitin affinity column. Western blot analysis was done and ubiquitinated proteins were detected with anti-ubiquitin antibody. Comparison of ubiquitylation band pattern of total proteins in R6 RNAi transformants and wild type *M. oryzae* B157 was done, and a prominent decrease in the number of bands of R6 was observed. The decrease in *MoSkp1* transcript level results in low level of MoSkp1 protein. The decreased level of MoSkp1 protein reduces the ubiquitination of proteins (Fig. 22). This further leads to various physiological conditions in silenced lines of *M. oryzae*. While it is clear from the above data in RNAi transformants that decrease of MoSkp1 protein in *M. oryzae* hindered development of infection structure appressoria, the cumulative effect of various proteins

with decreased ubiquitination is likely to have additional morphological, developmental and physiological effects.



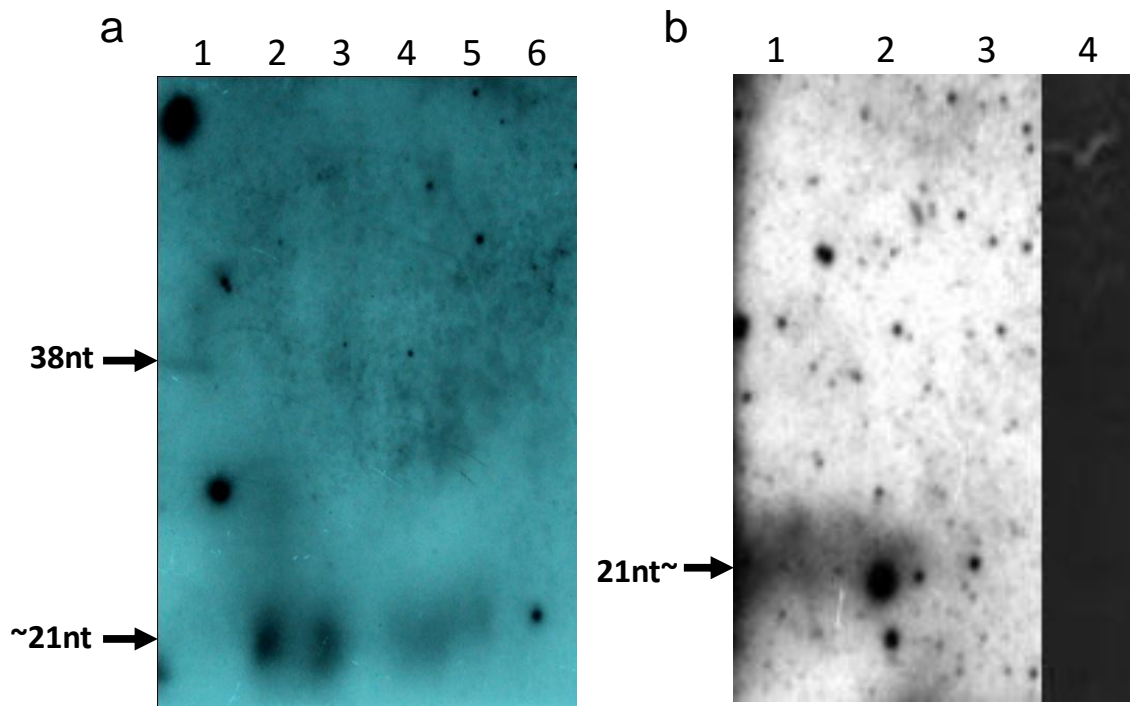
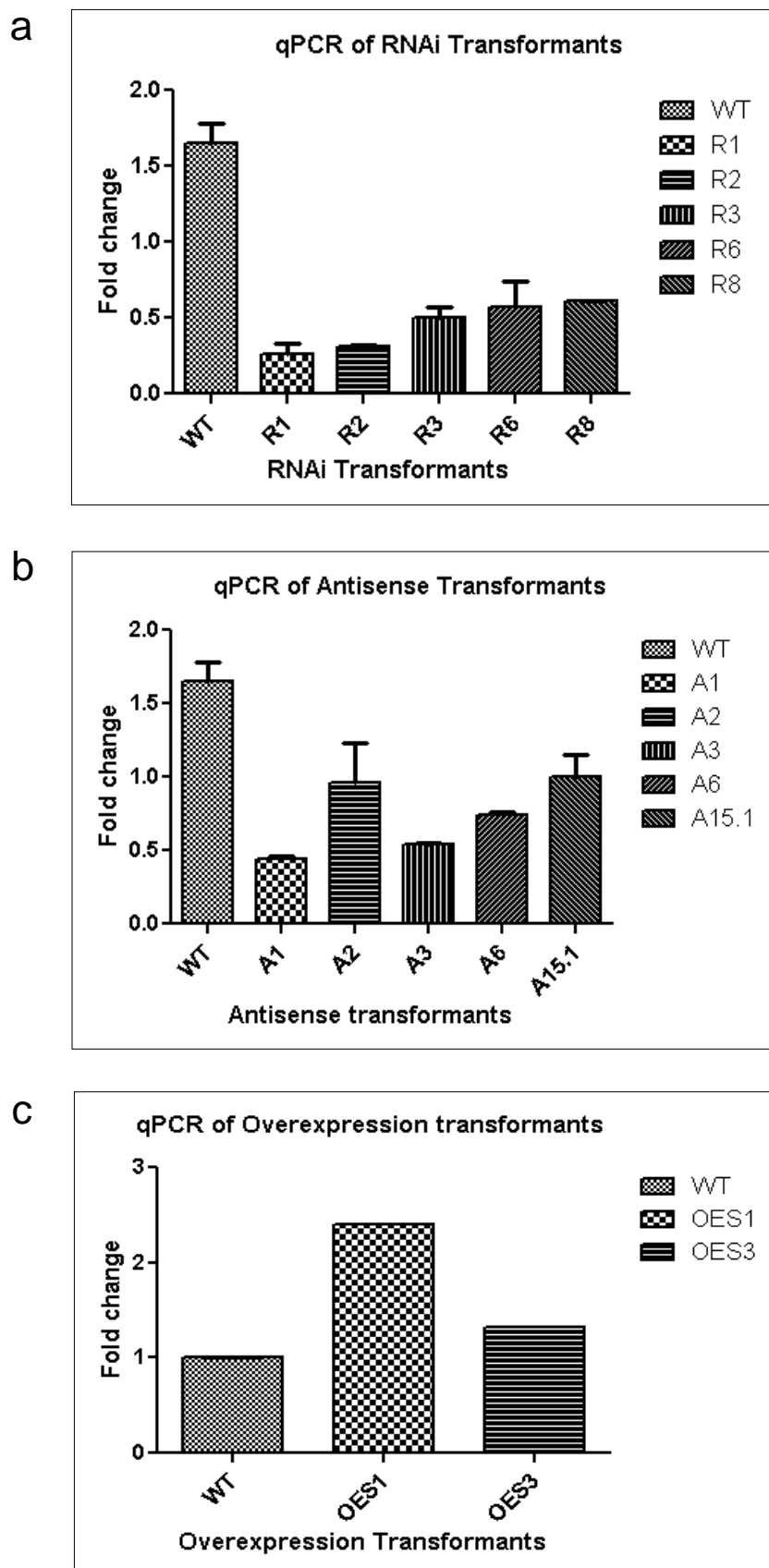


Figure 19: Southern hybridisation of *Skp1* RNAi transformants and antisense transformants. **(a)** Genomic DNA was isolated from five *MoSKP1* RNAi transformants and digested with *HindIII*. **(b)** Genomic DNA of four *MoSKP1* antisense transformants was digested with *XbaI*. **(c)** A 350 bp fragment of *TrpC* promoter was used as probe which is present in pSilent as well as in pSD2 vector

Figure 20: siRNA detection of *MoSKP1* RNAi transformants and *MoSkp1* antisense transformants. **(a)** Northern blot analysis of RNAi transformant showing small RNA of *MoSkp1*. Lane 2-5 contains R1, R2, R6 and R8 RNAi transformants, lane 1 is a 38 bp *MoSkp1* primer and lane 6 is with wild type *M. oryzae* B157 small RNA where no *Skp1* specific siRNA was detected. **(b)** Two transformants of *MoSkp1* antisense A15.1 and A6 in lane 1 and 2, lane 3 is wild type B157 and lane 4 has a 10 bp ladder



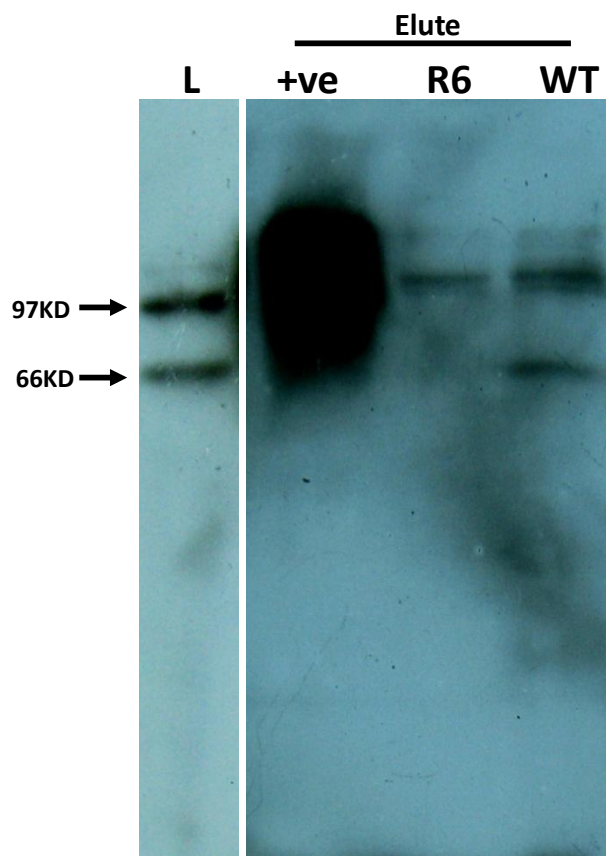


Figure 21: (a) qPCR analysis of *MoSKP1* RNAi transformants showing relative expression of transcript level of Skp1 transcript. The transcript level of Skp1 in transformants was found to be decreased by 90%. (b) qPCR analysis of *MoSKP1* antisense transformants. Three transformants showed decreased relative expression of *MoSKP1* transcript in comparison to wild type Skp1. (c) qPCR analysis of *MoSKP1* over-expression transformants. T-test was performed using ANOVA for each experiment and level of significance was calculated keeping $p \leq 0.001$ and graph were generated in GraphPad Prism 5 software

Figure 22: Ubiquitination enrichment assay of *MoSKP1* RNAi transformants. R6 RNAi transformant showed decreased ubiquitination pattern compared to wild type B157 *M. oryzae* strain. Equal amount of total protein was loaded in each lane. First lane is positive control (provided by Thermo Scientific Pierce, USA). Lane 'L' contains protein marker (97.4 -14.4kDa) (Bangalore Gene, India)

3.19 Western blot analysis of the MoSkp1 transformants

Western blot analysis was performed with the knockdown transformants to check the level of Skp1 protein. It is important to maintain the protein level in those transformants that show slow growth, less sporulation and are unable to form infection structures. In this context, five *MoSKPI* RNAi transformants and three antisense transformants were chosen for western blot analysis. Total protein was isolated from RNAi, antisense transformants and wild type *M. oryzae* and quantified by Bradford method. A 12% SDS-PAGE was run to separate proteins on the basis of their molecular weight, with 20 µg of total protein loaded in each lane. Purified Skp1-6xHis protein was also loaded as a positive control. Separated protein was then transferred to the PVDF (Hybond P+, Amersham, USA) membrane by wet transfer. The blot was blocked for 1 h in blocking solution of 3% skimmed milk in PBS solution. A polyclonal Anti-Skp1 antibody developed in Rabbit was used as primary antibody. After 1 h of incubation in primary antibody, the blot was washed and incubated in secondary antibody. Horseradish peroxidase conjugated Anti-IgG raised in goat was used as secondary antibody (dilutions 1:10000). The blot was developed by using the substrate 3,3'-Diaminobenzidine (DAB), Cobalt chloride and Hydrogen peroxide (Fig. 23 a&b).

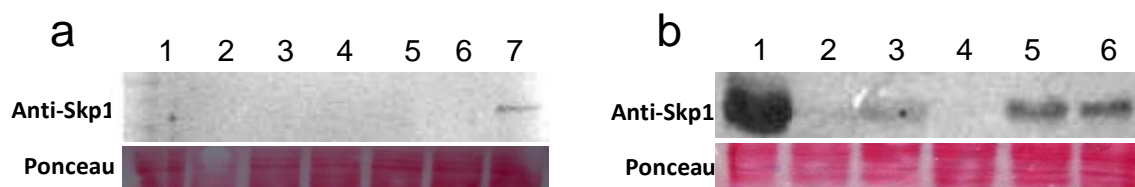


Figure 23: Western blot analysis of *MoSKP1* RNAi and antisense transformants. **(a)** Total protein was isolated from RNAi transformants and 20 μ g total protein was loaded in each lane. Protein levels were estimated using MoSkp1 antibody. **(b)** Levels of MoSkp1 protein in antisense transformants were analysed by western blot analysis by probing with Anti-MoSkp1 antibody. Equal loading of protein in each lane was confirmed by Ponceau S staining

Phenotypic characterisation of RNAi and antisense transformants

3.20 Infection assay and onion epidermis assay of RNAi transformants

Spray inoculation assay was performed using three RNAi transformants showing reduced level of transcript in real time experiment, namely, R1, R6 and R8 and the same were kept for the onion epidermis assay to check the penetration and appressorial development. The transformants were slow in germinating and were unable to form appressoria. One of the transformants was unable to grow even after 12 h (Fig. 24).

3.21 Localisation of MoSkp1 protein in wild type

For the localisation study, Skp1 antibody was used as primary antibody and anti rabbit IgG-TRITC conjugate was used as secondary antibody. As expected the Skp1 protein showed cytoplasmic localisation (Fig. 25). The staining was done at different stages of spore development. It was observed that MoSkp1 protein was found to be in the cytoplasm of the cell and mobilised from spore to the developing appressoria through the germ tube. Considering the information from the previous experiment that Skp1 is involved in the cell cycle, the localisation study also indicates that MoSkp1 is predominantly present in actively dividing cells of *M. oryzae*.

3.22 Expression profiling of Skp1 protein in wild type *M. oryzae*

An experiment was performed to investigate the levels of MoSkp1 protein at different time intervals. Expression profiling was done by inhibiting the cell cycle of *Magnaporthe* and then releasing it from arrest. Wild type *M. oryzae* B157 cells were arrested in S-phase by treating with hydroxyurea (2 mM) for 6 h and then cells were released by

washing out the hydroxyurea from media. Samples were collected at regular interval of 1 h, protein was isolated and western blot analysis was performed using Skp1 antibody. The expression of MoSkp1 was found to be increased after every 1 h (Fig. 26). The cells were arrested in S-phase at 0 h, where MoSkp1 was found to be expressed at very low levels and after releasing from arrest the expression of MoSkp1 increased upto 5 h, indicating the involvement of MoSkp1 in the cell cycle progression.

3.23 Sporulation assay and qPCR of various RNAi and antisense transformants

RNAi, antisense and overexpression transformants were checked for their sporulation and compared with the wild type strain *M. oryzae* B157. After growth for eight days on sporulation media oat meal agar (OMA), spores were isolated and counted in a Neubauer counting chamber. RNAi transformants (R1, R2, R3, R6 and R8), and antisense transformants (A1, A2, A3, A6 and A15.1) were both drastically reduced in sporulation, whereas the overexpression transformant OES1 had sporulation comparable to the wild type *M. oryzae* B157. In both cases of MoSkp1 knockdown, sporulation was found to be in the range of 1×10^4 spore/ml/cm² when compared with wild type strain and OES1 which had 1×10^6 spore/ml/cm² (Fig. 27, Table 2). A qPCR analysis was performed to quantify the level of transcript in the various transformants. In qPCR analysis it was found that transcript level of MoSkp1 was very low in both types of knockdown transformants whereas in OES1 it was elevated 2.4 fold (Fig. 21c). It is assumed that reduction in transcript level in the various knockdown transformants resulted in the reduced sporulation and other morphological defects.

3.24 Appressorial assay and conidial septa formation

Appressorial assay was performed for RNAi transformants but no proper appressoria development was observed in the transformants and so they were unable to breach the leaf cuticle. On closer examination of the conidial morphology, and it was found that the knockdown transformants (both RNAi and antisense transformants) were defective in their septa formation in spores. About 80% spores were having single septa or no septa in most of the transformants (Fig. 28). 25% of the total conidia produced by the *MoSkp1* RNAi transformants were found to contain single septum whereas the percentage of conidia without septum was highest in R1 transformant with 25%. Only 10% spores of *MoSkp1* RNAi transformant R1 were able to form appressoria on hydrophobic surface. *MoSKP1* antisense transformant A15.1 showed elongated germ tube developing from 75% spores, whereas no germination was observed in 60% spores of RNAi R1 transformant. This observation provides support to the hypothesis that reduction of *MoSKP1* transcript leads to reduced sporulation, defective spore morphology and reduced growth which finally leads to no appressorial development but instead leads to formation of elongated germ tube.

3.25 *MoSKP1* overexpression transformants show enhanced appressoria development

Wild type B157 strain was transformed with overexpression construct of *MoSKP1* and the transformants were checked for growth, sporulation and appressorial development. The *Skp1* transcript level of overexpression transformant (OES1) was 2.4 fold higher; growth and sporulation were comparable to B157 strain on complete media (CM) (Fig.

29 a&b). The efficiency of appressoria formation in OES1 transformant was increased compared to B157 strain. It was observed that the length of germ tube between conidia and appressoria was reduced in OES1 developing appressoria. About 80% of germ tubes measured were 15 μm or less than 15 μm in OES1 whereas in B157 strain only ~30% appressoria showed smaller germ tube (Fig. 29 c&d). This result shows OES1 enhances development of appressoria. Microscopic examination of MoSkp1 knockdown and overexpressed transformants revealed that single conidia were present on each of the conidiophores of RNAi transformants as opposed to wild type *M. oryzae* B157 and OES1 (Fig. 29e). This indicates that reduced levels of MoSkp1 results in reduction of sporulation, growth, appressorial development and septa defect in the transformants whereas the OES1 remain unaffected with respect to sporulation (Table 2).

3.26 Calcofluor staining and phenotypic study of RNAi transformant

Calcofluor was used to stain chitin deposition and it was found to be irregular in the transformant when compared to the wild type strain of *M. oryzae* B157. Spores of most of the *MoSKPI* RNAi transformants spores were devoid of chitin deposition (Fig. 30a). Septa formation was also affected in spores. Further, these transformants showed less melanin and reduced growth.

3.27 Nuclear and chitin staining of RNAi transformants

Nuclear status of the RNAi transformants was examined using Hoechst stain. It was found that the nucleus was disorganised and diffused in RNAi transformants. Simultaneous staining of chitin was able to identify that nucleus was disorganised and

there was no septa formation (Fig. 30b). This indicates that the cells remain arrested in the cell cycle and are unable to develop further. However, it is clear from the phenotype that completion of cell cycle is necessary for the development of appressoria and transformants are unable to do so.

3.28 Cell wall integrity assay

Cell wall integrity of all the transformants was checked by growing on the cell wall disrupting agents such as Caffeine (2.5 mM), Congo Red (2 mg/ml) and CFW (200 mM). RNAi and antisense transformants were unable to grow on CFW and Congo Red. There was growth on caffeine but it was less compared to B157 and OES1 (Fig. 31, Table 3). Cell wall integrity assay again confirms the defects in cell walls of knockdown transformants.

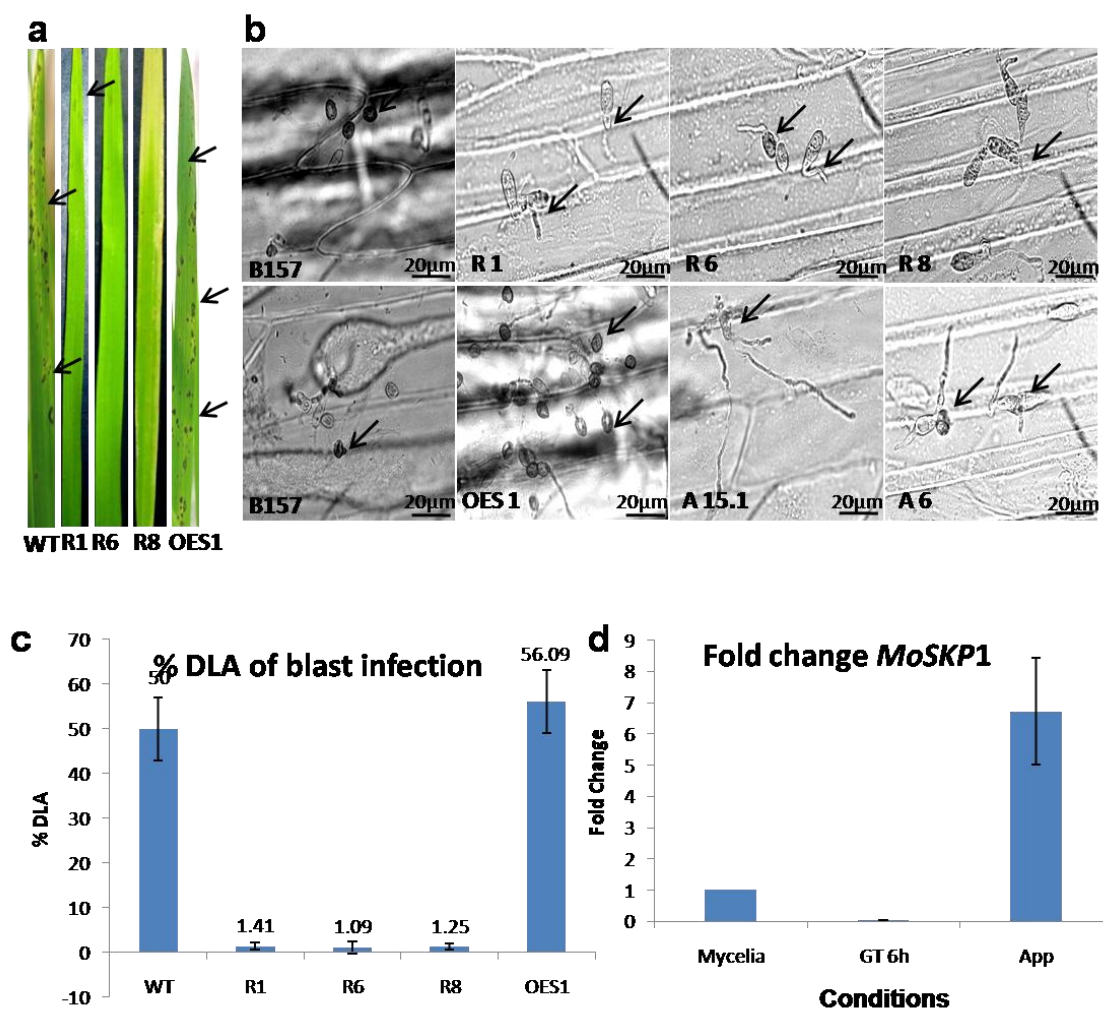


Figure 24: *MoSKP1* RNAi transformants are unable to infect rice leaves and cannot penetrate onion epidermis. **(a)** Spore count was maintained at 1×10^4 / ml for each transformant and spray inoculation was applied to 21 days old CO-39 rice line. After seven days, the severity of infection was measured. **(b)** Onion epidermis assay was performed taking RNAi, antisense and over-expression OES1 transformants. After 12 hour of inoculation, samples were observed under microscope at 100x magnification. **(c)** Percentage disease leaf area was calculated for infected rice leaves. **(d)** Real time PCR for mycelia, germ tube grown for 6 h and mature appressoria.

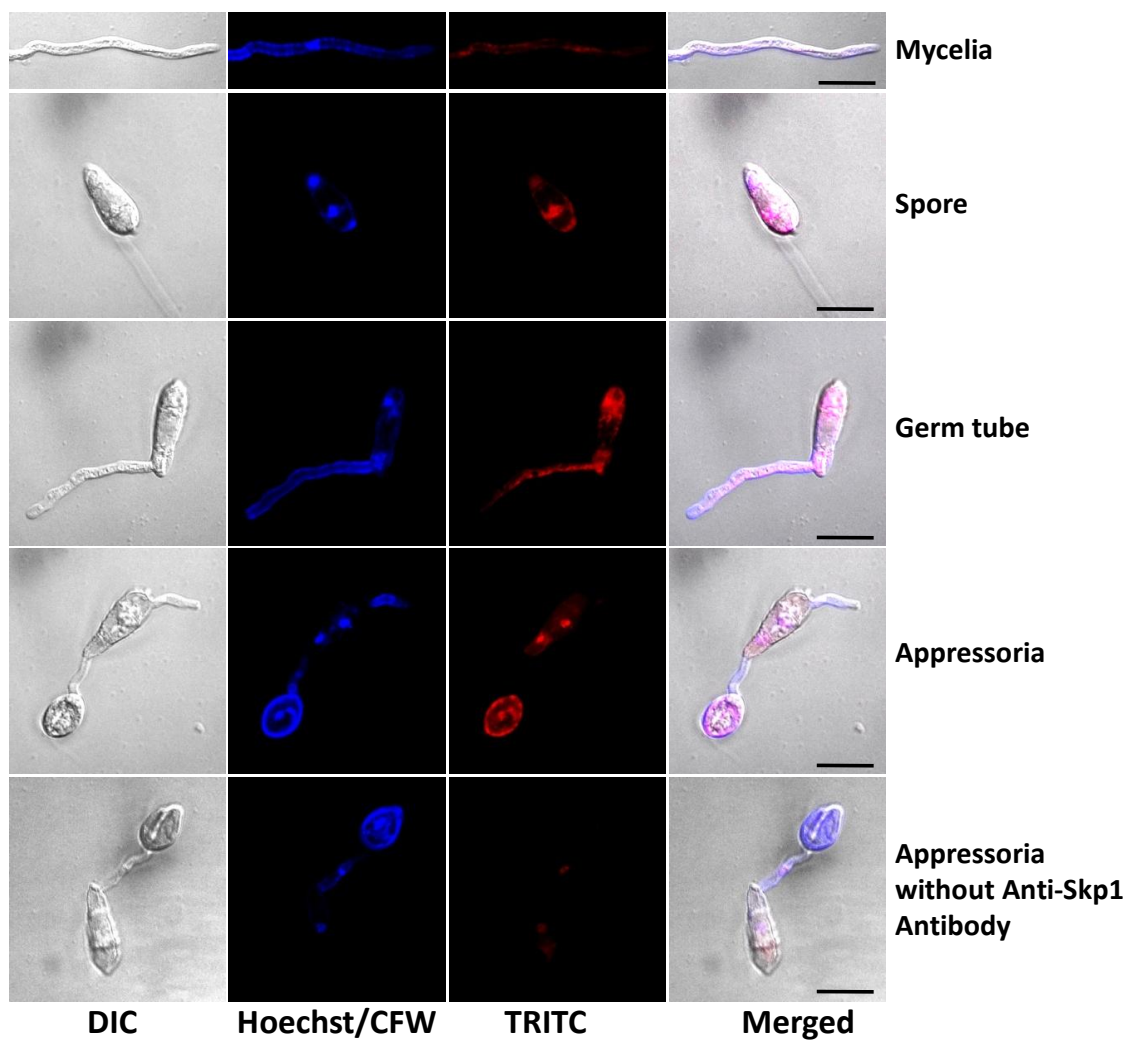


Figure 25: Subcellular localisation of MoSkp1 protein in *M. oryzae* B157. MoSkp1 localisation was studied in spore (upper panel), germ tube (middle panel) and appressoria (lower panel) by immunostaining using anti-Skp1 antibody and TRITC conjugated secondary antibody. In the spore, MoSkp1 co-localises in cytoplasm. As the spore germinates, MoSkp1 is enriched in the germ tube and reduced in spore cells. After appressoria development MoSkp1 was found to localise in appressoria. Calcoflour White and Hoechst 3342 stain were used to stain chitin and nucleus respectively

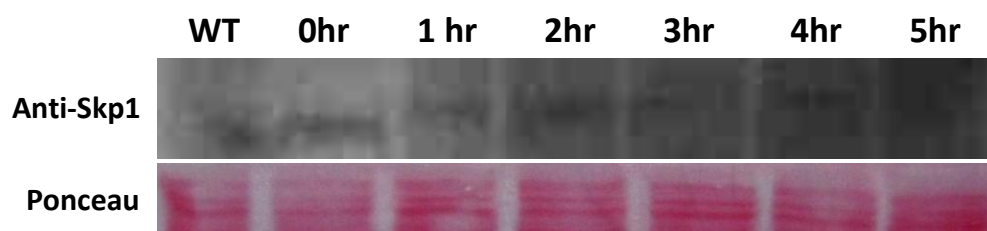
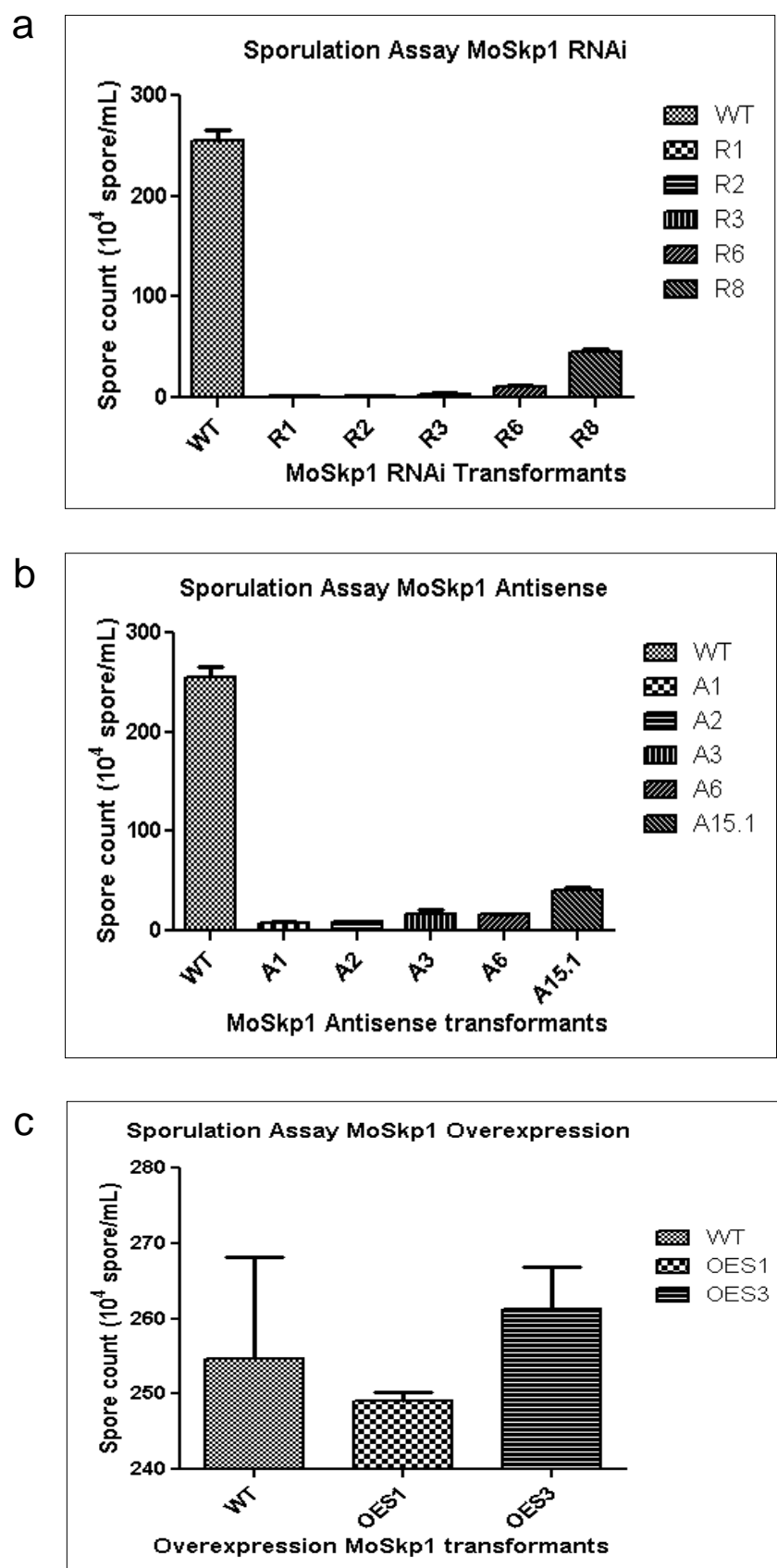


Figure 26: Expression profiling of MoSkp1 protein in *M. oryzae*. Lane 1 contains untreated wild type *M. oryzae* B157 protein. Lane 2-7 contains total proteins of *M. oryzae* B157 treated at intervals of 1 h with the cell cycle arresting drug Hydroxyurea at a final concentration of 200 μ g/ml. Anti-Skp1 antibody was used as primary antibody



Figure

27:

Sporulation assay of knock-down and over-expression transformants. Sporulation assay was done on 8th day of inoculation. Graph with Y-Axis being spore count in 1×10^4 /ml/cm². **(a)** Sporulation assay of RNAi transformants. **(b)** Sporulation in *MoSkp1* Antisense transformants. **(c)** Sporulation assay in *MoSkp1* over-expression transformants. T-test was performed using ANOVA for each experiment and level of significance was calculated keeping $p \leq 0.001$ and graph were generated in GraphPad Prism 5 software

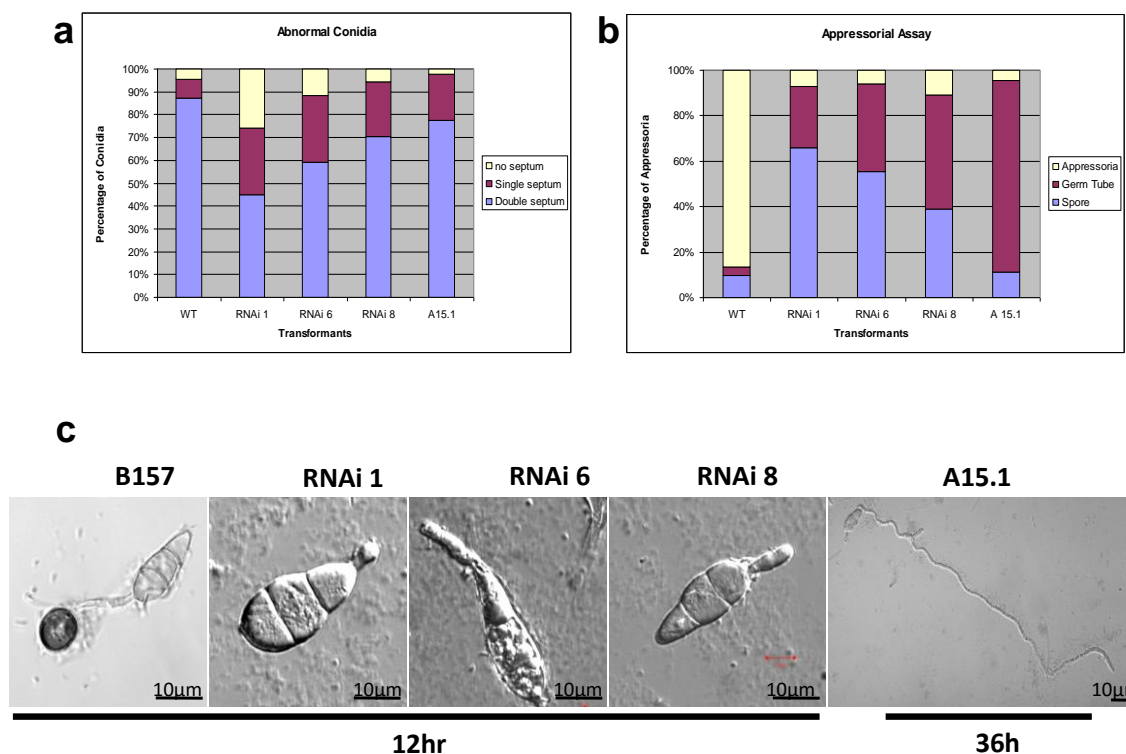


Figure 28: Abnormal conidiation and less appressoria formation in *MoSKP1* RNAi and antisense transformants. **(a)** Abnormal conidia formation with no septa, single septa and double septa was observed in RNAi transformants R1, R6, RNAi 8 and in antisense A15.1 transformants. **(b)** Appressoria formation efficiency was checked for knock-down transformants and graphs was generated. Experiment was performed in triplicate taking 100 spores in each case. **(c)** Representative picture of appressorial assay for transformant after 12 and 36 hours

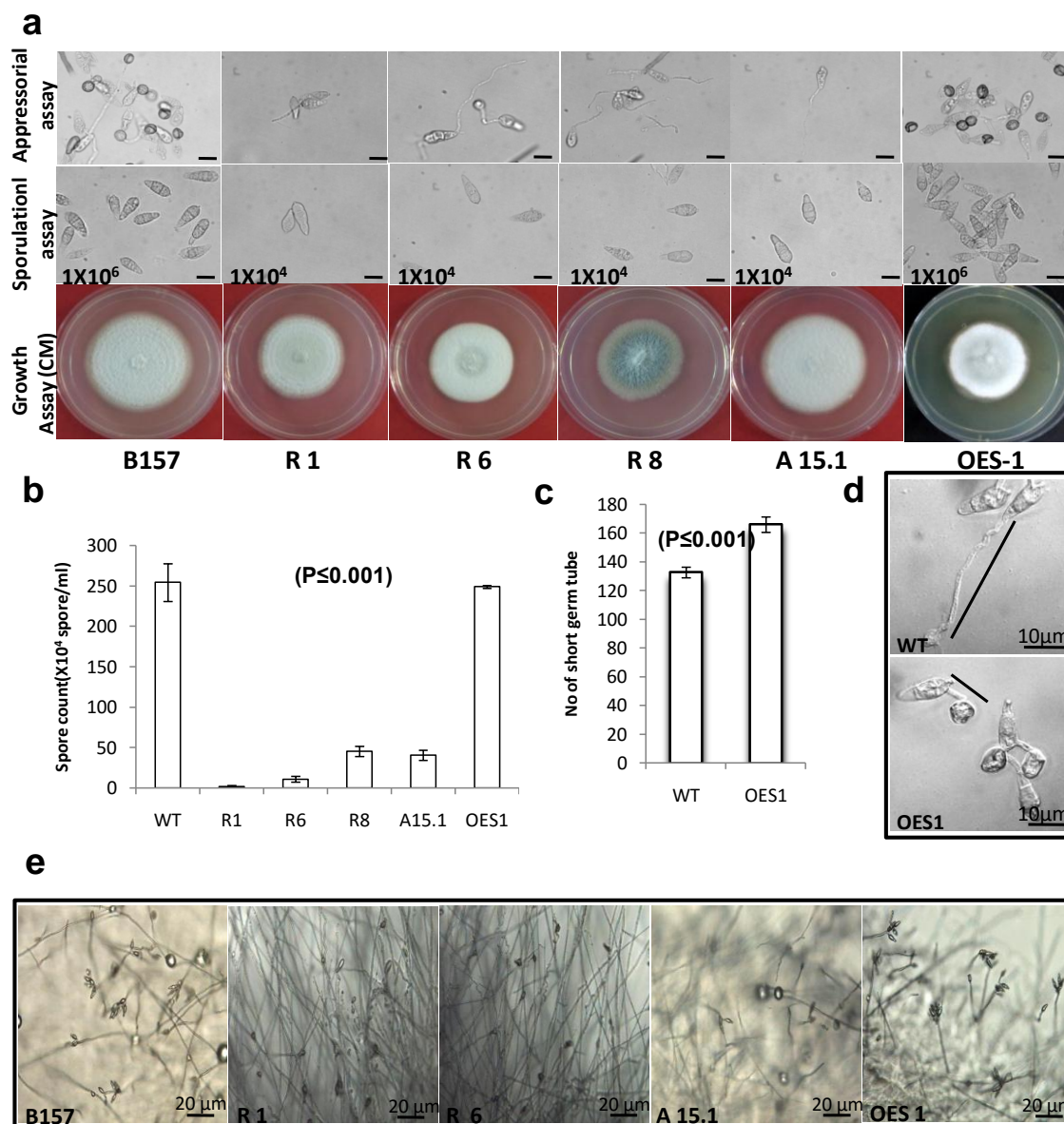


Figure 29: Growth, sporulation and appressorial assay of *MoSKP1* transformants. **(a)** Growth of the transformants was checked on Complete Media (CM) for 7 days, sporulation was checked after 8 days post inoculation on Oat Meal Agar (OMA) and the ability to form appressoria was assayed on hydrophobic cover glass. **(b)** Sporulation efficiency of transformants was quantified ($P < 0.001$). **(c)** Length of germ tube between spore and appressoria were measured in OES1 transformant and compared with B157. 200 appressoria was counted and number of smaller germ tube ($\leq 25 \mu\text{m}$) was calculated at significant level ($P < 0.001$). **(d)** Micrograph showing length of germ tube in OES1 transformant and B157 strain. Bar=10 μm . **(e)** Arrangement of conidia on conidiophores showing the decrease in sporulation in RNAi and antisense transformants

Table 2:

Strain	Mycelial growth ^a (mm)	Conidiation ^b (10 ⁴ per ml)	Conidial germination ^c (%)	Double septa conidia ^d (%)	Single septa conidia ^e (%)	No septa conidia ^f (%)	Appressorium formation ^g (%)
WT	66±1.41	254.66±23.35	90.33±4.50	88±2.64	8±2	4.66±0.57	86.33±5.13
RNAi 1	41.5±2.12	2±1	34±5.29	44.66±4.50	29±1	25.66±3.78	7±4.35
RNAi 6	40±1.41	11±3.60	44.66±5.03	59±1	29.33±1.15	11.66±2.08	6±3.6
RNAi 8	43.5±2.12	45.33±6.42	61±1	70.33±1.52	24±3.60	5.66±2.51	11±1.73
A 15.1	51±1.41	40.66±6.11	88.66±3.21	77.66±2.51	20±1	2.33±2.30	4.33±1.15
OES1	66.5±0.70	249±2	96.33±0.57	94±1	4±1	4.66±1.52	96.66±1.52

Table2: Comparison of mycological characteristics among various transformants. Statistical analysis was performed using Anova at significant value $P \leq 0.001$. ^aGrowth was measured as diameter of mycelium 7 days after inoculation. ^bConidiation assay was performed by isolating conidia in 1ml of sterile water from the same plate used for growth measurement. ^cGermination ability was measured as the ratio of germinating conidia to total conidia. ^{def} Septation was counted after staining with CFW stain. Out of 100 conidia, the number with double septa, single septa and no septa were counted. ^gAppressoria formation was measured as the ratio of appressorium forming conidia to germinating conidia on hydrophobic coverslips

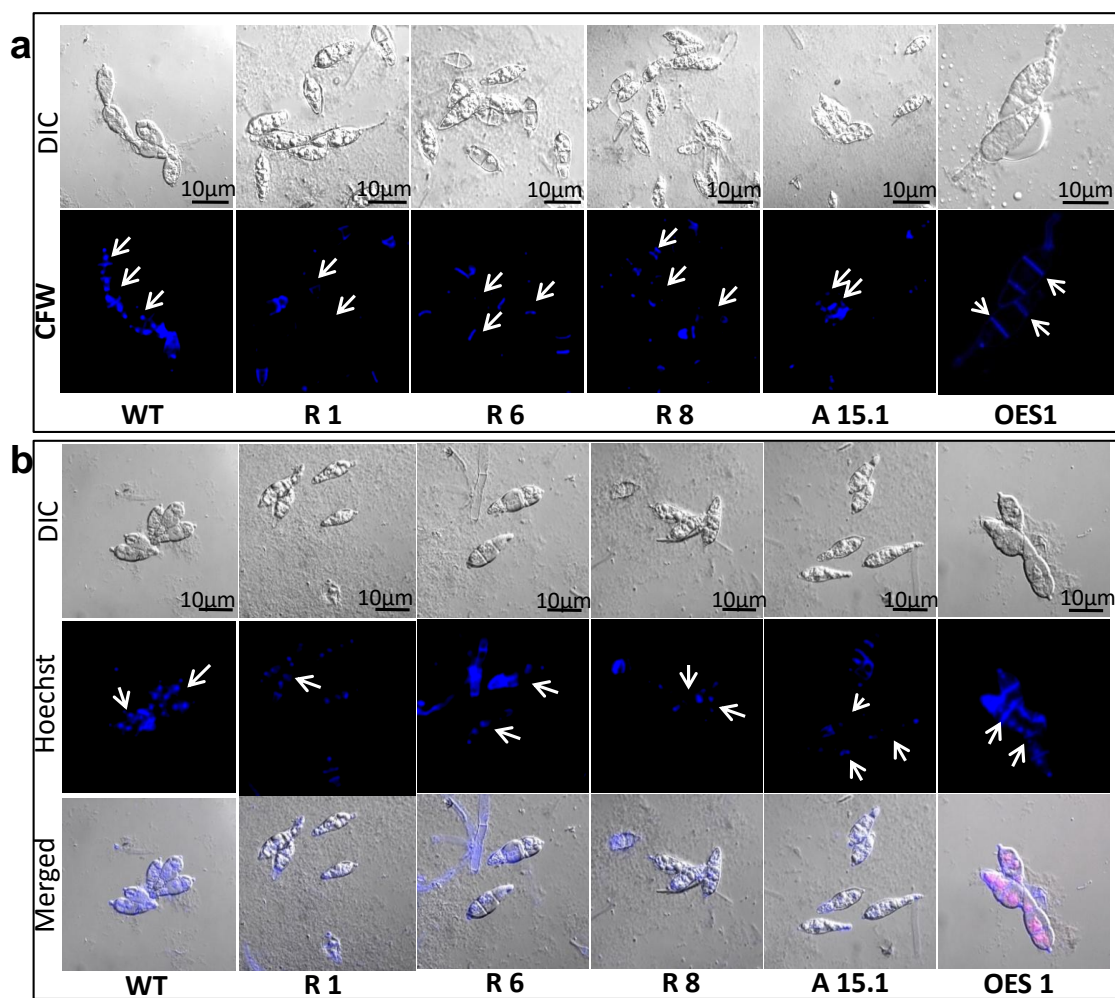


Figure 30: Defective septation and nuclear disorganisation in conidia of *MoSKPI* RNAi and antisense transformants. **(a)** Calcofluor White stain was used to stain chitin and conidial cell septum of the transformants. Arrow indicates the absence of septation in RNAi transformants. **(b)** Hoechst staining of knockdown transformants was done to see the nuclear organisation in the defective spores. Arrow indicates the diffused and disorganised nucleus in the transformants.

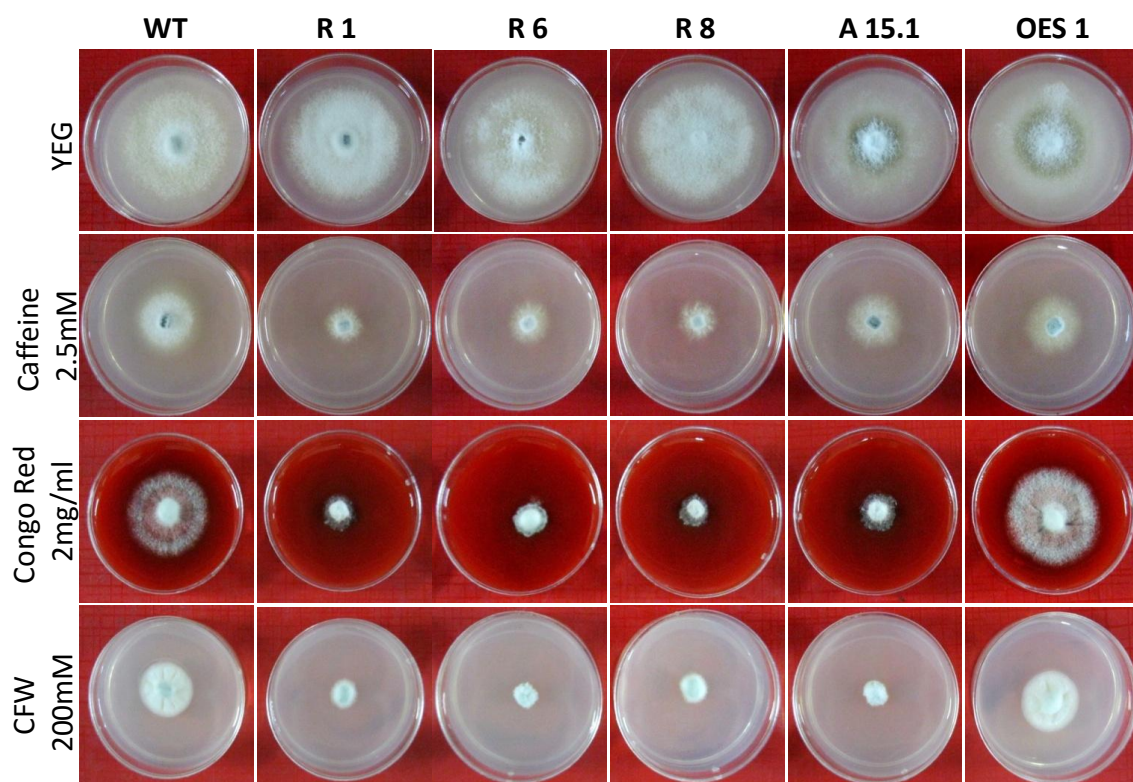


Figure 31: *MoSKPI* RNAi and antisense transformants were defective in cell wall integrity. Cell wall integrity of transformants was checked by growing on Yeast extract glucose agar (YEG) media containing Caffeine (2.5 mM), Congo red (2 mg/ml) and Calcofluor White (200 mM). Inocula were 2 mmX2 mm mycelia plug for each culture and diameter of growth was measured after 5 day. The experiments were performed in duplicate.

Table 3:

Strain	YEG (mm)	Caffeine (2.5mM) (mm)	Congo Red (2mg/ml) (mm)	CFW (200mM)(mm)
WT	26±1.41	12.5±0.70	16±1.41	9.5±0.70
R1	27±1.41	4.5±0.70	3.5±0.70	3.5±0.70
R6	28.5±0.70	3.5±0.70	4±1.41	3±0.0
R8	28.5±0.70	4.5±0.70	4±0.0	3.5±0.70
A15.1	28±0.0	6.5±0.70	4±1.41	3±0.0
OES1	28±0.0	7.5±0.70	18±0.0	11.5±0.70

Table 3: Comparison of mycelia growth of *MoSKPI* RNAi and antisense transformants in presence of cell wall disrupting agents. Growth was measured as the diameter of mycelium 5 day after inoculation.

3.29 Interaction Study of Skp1

Skp1 interacts with a number of F-box proteins in the cell during the S-phase. Interaction ability of MoSKP1 with F-box protein was checked by yeast two hybrid assay. Based on bioinformatics analysis and literature survey, one of the F-box protein was selected (MGG_06351.5, a hypothetical protein) for the yeast two hybrid assay. MGG_06351.5 is homolog of Frp1 protein and involved in pathogenesis in *F. oxysporum* (Duyvesteijn *et al.* 2005). Total RNA was isolated and cDNA was synthesised by reverse transcriptase. cDNA of Skp1 and putative F-box protein was cloned into a bait vector pGBKT7 and prey vector pGADT7 respectively. After co-transformation of recipient *S. cerevisiae* culture AH109 with the two vectors, the colonies appearing on the selection plate were further analysed for the interaction. Colonies which were able to grow on Quadruple dropout media (SD Ade⁻/ His⁻/ Leu⁻/ Trp⁻) were expected to show interaction because only interaction between MoSkp1 and MoFrp1 will lead to the expression of *Ade* gene, which is very tightly regulated. Further, total protein was isolated from the colonies which were growing on the selection plate and western blot analysis was done to show the presence of interacting protein in the cell. Interaction was further confirmed by the co-immunoprecipitation assay. The tagged proteins were isolated from the recipient *S. cerevisiae* culture AH109 and allowed to interact *in vitro*. Further, to identify the interacting proteins a pull down experiment was done by using protein A affinity chromatography. Western blot analysis confirmed the presence of interacting protein using anti-HA antibody as primary antibody (Fig. 32).

3.30 Pull down Analysis

In order to find interacting protein with MoSkp1 a pull down assay was performed using 6XHis-MoSkp1 protein as bait and total protein of *M. oryzae* as prey. Skp1 is the central protein in SCF complex and it is believed that it performs various functions in the cell, so it is of interest to identify the other interacting partners of this protein to better understand the role of Skp1. The pull down protein and peptide mass finger printing results confirmed that MoSkp1 is a SCF E3 ligase subunit and involved in the SCF complex formation along with other interaction such as with proteins like RNA polymerase II subunit. Most of the protein in this experiment was found to be hypothetical and uncharacterised (Fig. 33, Table 4).

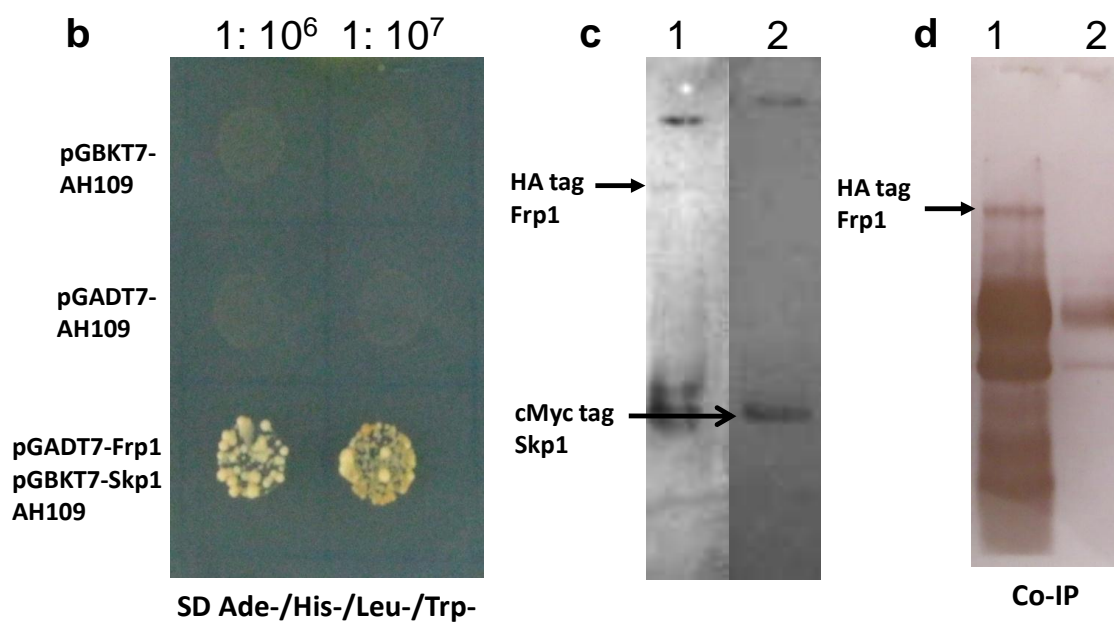
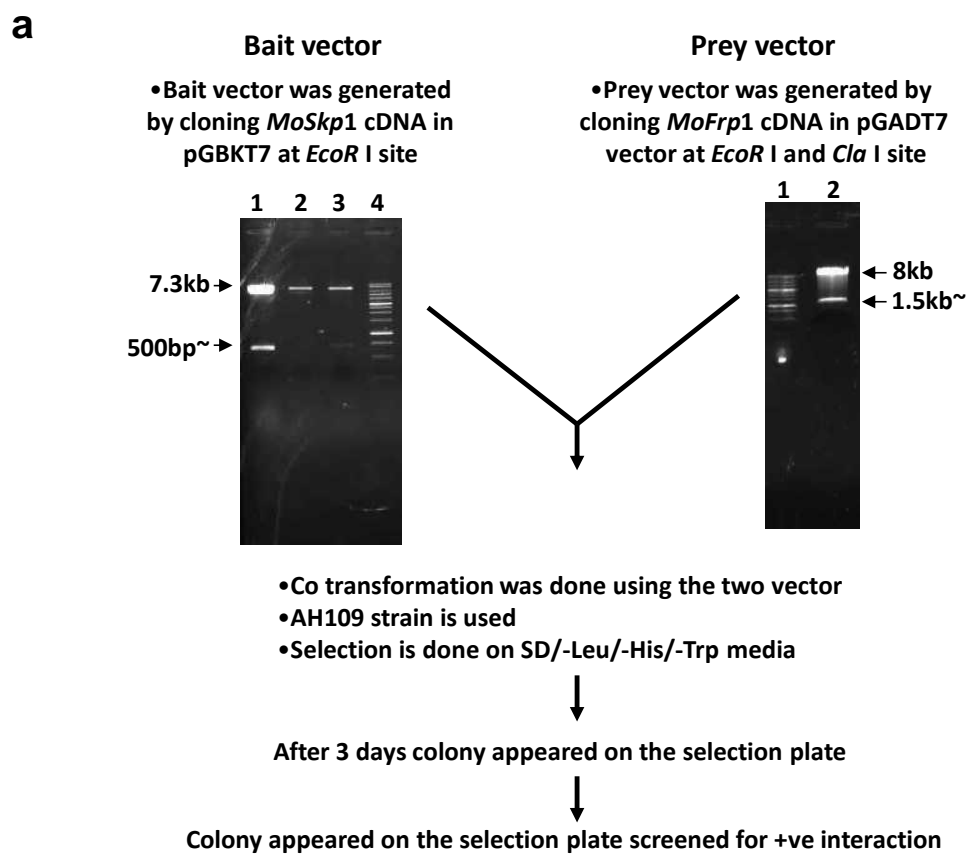


Figure 32: Yeast two hybrid assay to show the interaction between *MoSkp1* and *MoFrp1*. (a) *MoSKP1* was cloned in pGBKT7 and *MoFRP1* was cloned in pGADT7 vector and was confirmed by restriction digestion. (b) Growth of colonies after co-transformation on Quadruple dropout media. (c) Western blot analysis to show the presence of interacting protein. anti-HA and anti-cMyc were used as antibody. (d) Pull down of interacting protein using protein A resin and western blot analysis using primary anti-HA antibody

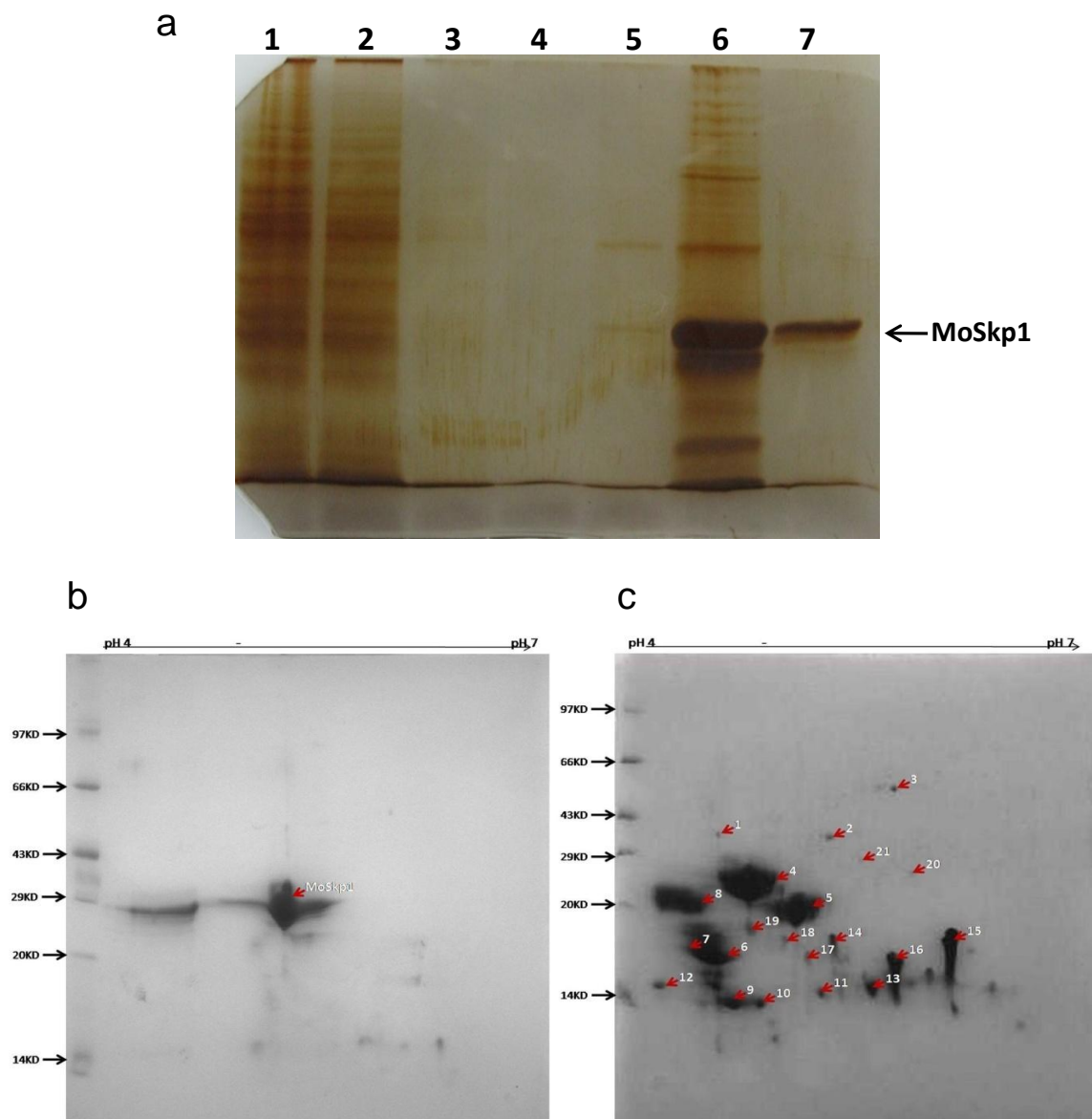


Figure 33: SDS-PAGE of pull down protein, stained with Silver nitrate. (a) Lane 1 contains Flow through, Lane 2 contains 1st wash, Lane 3 contains 2nd wash, Lane 4 contains 3rd wash, Lane 5 contains 1st eluate, Lane 6 contains 2nd eluate and Lane 7 contains 3rd eluate. (b) 2D gel analysis of expressed *MoSkp1* protein as control (c) Gel

showing pull down protein along with MoSkp1 tagged protein. Red circle indicate purified MoSkp1 tagged protein

Table 4:

S.No.	Hit found in PMF	Detail of gene	Score	Detail and function
1	<i>Trichophyton tonsurans</i> CBS-112818	Putative uncharacterized protein (TESG_08531)	38.8	Hypothetical protein
2	<i>Botryotinia fuckeliana</i> B05.10	(BC1G_13955)	15.1	Hypothetical protein
3	<i>Saccharomyces cerevisiae</i>	AWRI1631 – Pir3 gene Sc,AWRI1631_110670	15.1	Hypothetical protein
4	<i>Ajellomyces capsulatus</i>	(NAm1)	16.2	Predicted protein
5	<i>Magnaporthe oryzae</i> 70-15		86.4	E3 ubiquitin ligase complex SCF subunit scon-3
6	<i>Hypholoma fasciculare</i>		18.3	RNA polymerase II largest subunit
7	<i>Phanerochaete carnosa</i>	PHACADRAFT_251149 HHB-10118-sp	13.5	Hypothetical protein
8	<i>Magnaporthe oryzae</i> 70-15		82.5	E3 ubiquitin ligase complex SCF subunit scon-3
9	<i>Ajellomyces capsulatus</i>	NAm1	14.5	Predicted protein
10	<i>Candida albicans</i>	CaO19.8758, SC5314	16.2	Hypothetical protein
11	<i>Colletotrichum gloeosporioides</i>	CGGC5_11939 Nara gc5	60	Hypothetical protein
Control	<i>Magnaporthe oryzae</i> 70-15	MoSkp1 expressed	80.3	E3 ubiquitin ligase complex SCF subunit scon-3

Table 4: List of proteins after Peptide mass finger printing of spots from pull down assay

3.31 Two dimensional protein analysis of MoSkp1-RNAi transformant

Differential protein expression in *MoSKP1* RNAi transformants R6 was checked. The R6 transformants showed low expression of *MoSkp1* transcript compared to wild type B157 strain in real time experiment and selected for 2D gel electrophoresis analysis. Total protein of R6 MoSkp1 RNAi transformant and wild type *M. oryzae* B157 was isolated and subjected to 2D gel analysis. Silencing of *MoSKP1* led to differential expression of total protein in R6 RNAi transformant. Decrease in the MoSkp1 transcript led to the down regulation of various proteins in RNAi transformant (Fig. 34). A total of 647 spots were detected, out of which 184 were found to be up regulated and 463 were down regulated.

3.32 *in Vitro* phosphorylation and dephosphorylation assay of MoSkp1 protein

Bioinformatics analysis indicates the presence of five putative phosphorylation sites in MoSkp1. NetPhos 2.0 Yeast tool at ExPASy software was used for the prediction of phosphorylation sites in the MoSkp1 (MGG_04978) protein sequence. The software predicted five serine and three threonine residues. Of the Ser residues identified (Ser¹⁸, Ser⁷⁷, Ser⁸¹, Ser⁸³ and Ser¹³⁶ with scores of 0.983, 0.998, 0.995, 0.996 and 0.998 respectively), three residues at positions **77**, **81** and **83** were the most probable target for phosphorylation. There are three sites of phosphorylation for threonine, of which two are present in vicinity of Serine residue at **76** and **86** positions with score 0.993 and 0.794 respectively (Fig. 35). Prediction was experimentally supported by performing *in vitro* phosphorylation and dephosphorylation assay with the recombinant MoSkp1 protein followed by Isoelectric focusing to separate the proteins. A shift was observed in

phosphorylated protein. The autophosphorylation ability of MoSkp1 was also checked. MoSkp1 was found to be phosphorylated and it then got dephosphorylated but did not show autophosphorylation (Fig. 36).

3.33 Hydroxyurea treatment of *M. oryzae* strain B157

Previous studies have shown that cellular differentiation, morphogenesis and development of appressoria in *M. oryzae* are tightly regulated by coupled mitosis and cytokinesis in the extending germ tube (Saunders et al., 2010, a&b). In order to compare the effect of cell cycle arrest and *MoSKP1* knockdown on development, the wild type B157 strain of *M. oryzae* was treated with Hydroxyurea (HU, 200mM), a known inhibitor of cell cycle progression that functions by inhibiting DNA replication and activating the checkpoint at G1/S phase (Singer and Johnston, 1981, Koc *et al.*, 2004). The wild type B157 strain of *M. oryzae* was unable to form appressoria after treatment with HU and showed development of germ tube comparable to *MoSKP1* RNAi and antisense transformants after a given interval of time (Fig. 37). Fission yeast *skp1* mutants have been shown to arrest either in G1 or G2 of the cell cycle, which leads to elongated cells (Bai *et al.*, 1996, Connelly and Hieter, 1996, Kaplan *et al.*, 1997, Skowyra *et al.*, 1997).

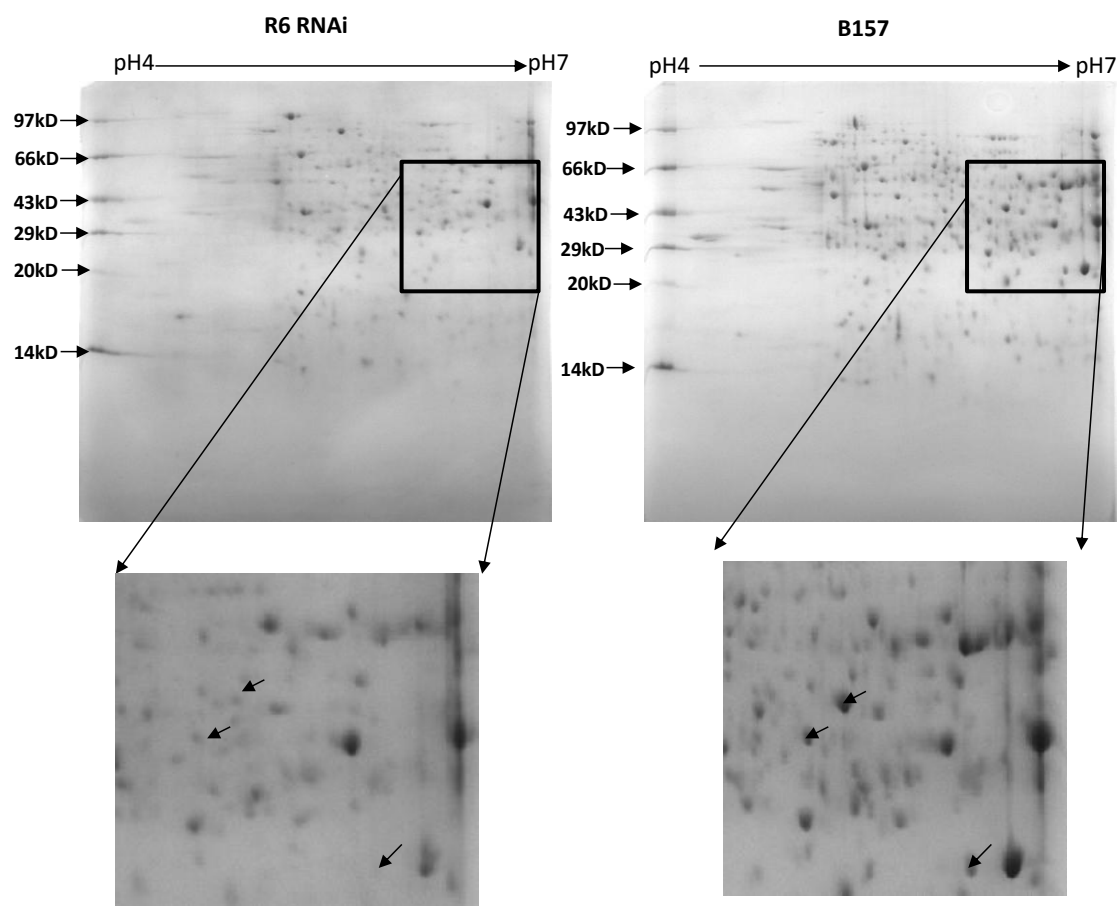
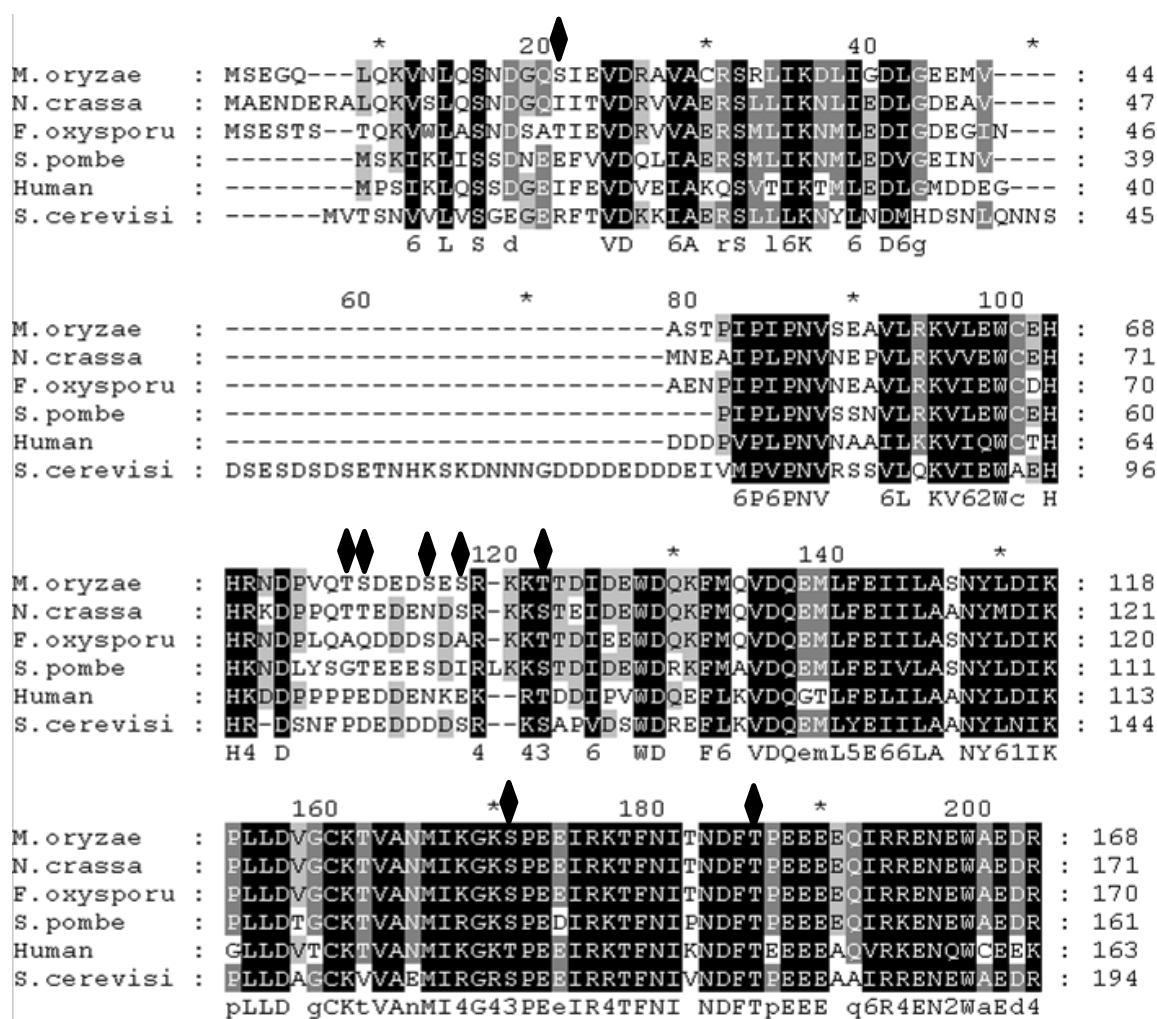


Figure 34: Two dimensional gel electrophoresis was performed using R6 RNAi transformants and the wild type *M. oryzae* strain B157. 647 spots were detected using PD Quest software (Biorad), 184 were up regulated and 463 spots were down regulated.



S-18, 77,81,83,136 ; T- 76,87,151 for MoSkp1

Figure 35: Multiple sequence alignment of Skp1 protein and bioinformatics prediction for phosphorylation sites using NetPhos 2.0 software. Trapezium indicates the most probable targets for phosphorylation

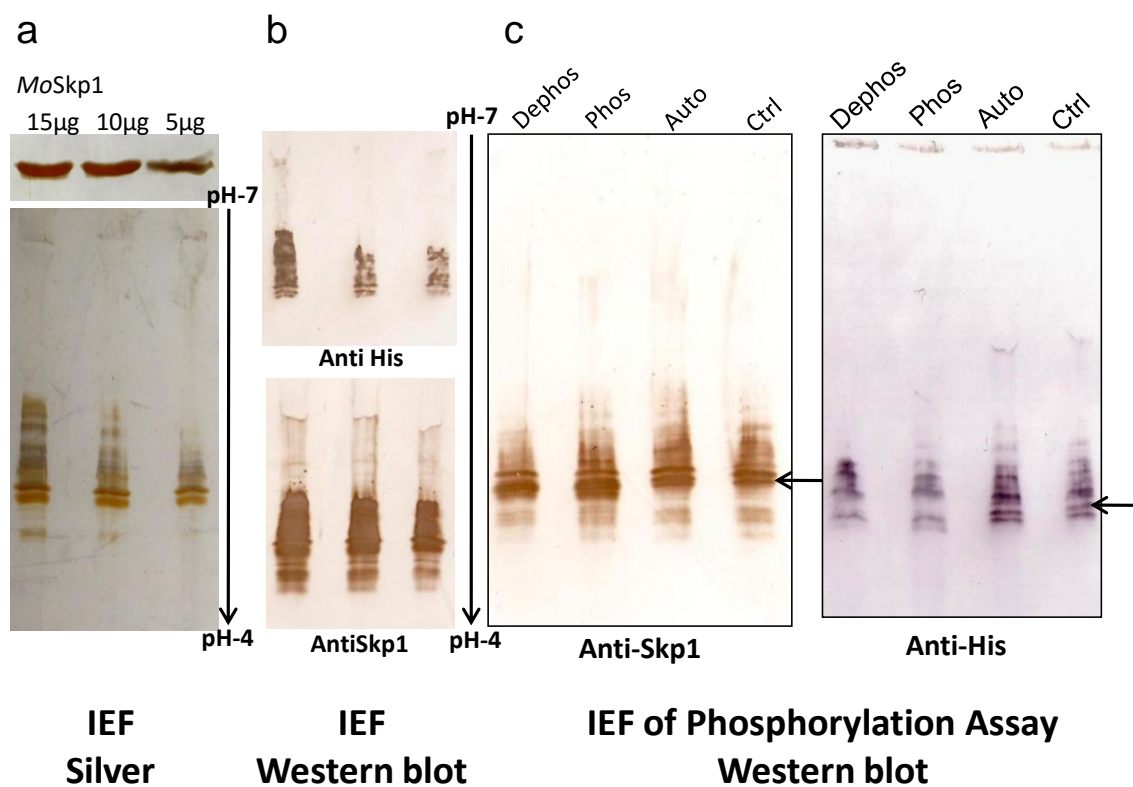


Figure 36: *In vitro* phosphorylation of recombinant MoSkp1 protein. (a) Different amounts of purified MoSkp1 protein were run on isoelectric focusing gel and silver staining was done. (b) Western blot analysis was done using anti-His antibody. (c) Western blot analysis was done using anti-Skp1 antibody. (d) Reaction mixture was run on IEF gel and transferred to PVDF membrane, followed by probing with anti-MoSkp1 antibody. (e) Similar blot was probed with anti-His antibody. Arrow indicates the shift in the band of interest.

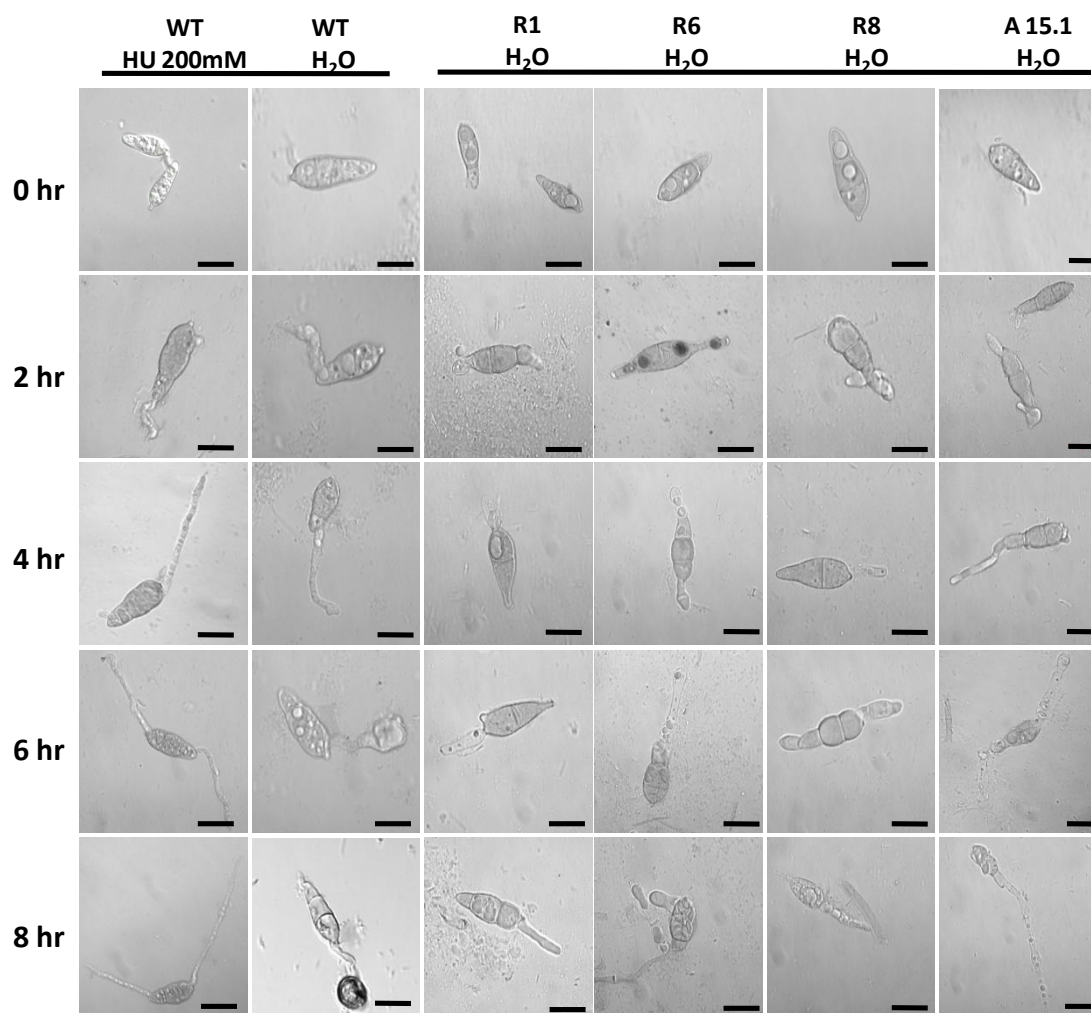


Figure 37: *MoSKP1* RNAi and antisense transformants were defective in cell cycle. A microscopic analysis of RNAi transformants and the wild type strain was performed at different time point of spore development. Wild type *M. oryzae* B157 strain was treated with Hydroxyurea (200 mM) and checked for appressoria formation for up to 8 h. *M. oryzae* B157 without hydroxyurea was taken as control. All the photographs were taken under laser scanning microscope at 63 X magnification (LSM700 Carl Zeis).